

The dynamics of higher-order novelties

Gabriele Di Bona^{1, 2, 3, 4}, Alessandro Bellina^{4, 5}, Giordano De Marzo^{4, 5, 6, 7}, Angelo Petralia⁸,
Iacopo Iacopini^{9, 10}, and Vito Latora^{1, 7, 11, *}

¹School of Mathematical Sciences, Queen Mary University of London, London E1 4NS, United Kingdom

²CNRS, GEMASS, 59 rue Pouchet, F-75017, Paris, France

³Sony Computer Science Laboratories Rome, I-00184, Rome, Italy

⁴Centro Ricerche Enrico Fermi, I-00184 Rome, Italy

⁵Dipartimento di Fisica Università “Sapienza”, I-00185 Rome, Italy.

⁶Sapienza School for Advanced Studies, “Sapienza”, I-00185 Rome, Italy.

⁷Complexity Science Hub Vienna, A-1080 Vienna, Austria

⁸Department of Economics and Business, University of Catania, I-95128 Catania, Italy

⁹Network Science Institute, Northeastern University London, London, E1W 1LP, United Kingdom

¹⁰Department of Network and Data Science, Central European University, A-1100 Vienna, Austria

¹¹Dipartimento di Fisica ed Astronomia, Università di Catania and INFN, I-95123 Catania, Italy

*Email: v.latora@qmul.ac.uk

ABSTRACT

Understanding how humans explore the world in search of novelties is key to foster innovation. Previous studies analyzed novelties in various exploration processes, defining them as the first appearance of an element. However, innovation can also be generated by novel association of what is already known. We hence define higher-order novelties as the first appearances of combinations of two or more elements, and we introduce higher-order Heaps’ exponents as a way to characterize their pace of discovery. Through extensive analysis of real-world data, we find that processes with the same pace of discovery, as measured by the standard Heaps’ exponent, can instead differ at higher orders. We then propose to model the dynamics of an exploration process as a random walk on an evolving network of the possible connections between elements. The model reproduces the empirical properties of higher-order novelties, revealing how the space of possibilities expands over time along with the exploration process.

Introduction

As humans, we experience novelties as part of our daily life. By the term *novelty* we generally indicate two apparently different things¹. On the one hand, we can think of a novelty as the first time we visit a neighborhood, enter a newly launched pub, or listen to a song from an artist we previously did not know. In this case, the novelty represents a discovery for a single individual of a place, an artist or, more in general, an item. On the other hand, there are discoveries that are new to the entire population, as could be a technological advancement or the development of a new drug. However, these two cases are not entirely distinct, as the second set of novelties, those new to everyone, represent just as a subset of the first one. Analysing how novelties emerge both at the individual level, and at the level of the entire population, is key to understand human creativity and the neural and social mechanisms that can lead to new discoveries and innovation.

The increasing availability of data on human behavior and consumption habits has allowed to study how humans explore the world, how novelties emerge in different contexts, and how they are distributed in time^{1–3}. Empirical investigations cover a broad range of different areas⁴ ranging from science⁵ and language^{6,7}, to gastronomy⁸, goods and products⁹, network science¹⁰, information¹¹, and cinema¹². No matter the topic, one can always represent data coming from real-world explo-

ration processes as sequences of items that are sequentially adopted or consumed¹³. In this way, the activity of a user of, for example, an online digital music platform is turned into a sequence of listened songs, and a novelty is defined as the first time a song, or an artist, appears in the sequence¹⁴. Analogously, articles published in a scientific journal can be turned into a time-ordered sequence of concepts or keywords discovered by the community, and a novelty can be defined, again, as the first-time appearance of a keyword³. Under this framework, evidence shows that—independently of the system they belong to—novelties seem to obey the same statistical patterns on the way they are distributed and correlated in time¹. In particular, most empirical sequences follow Heaps’^{15–17}, Zipf’s^{18–22}, and Taylor’s laws²³.

Along with data-driven investigations, a relevant scientific problem is that of finding plausible mechanisms to reproduce and explain the empirical observations. What are the rules controlling the appearance of new items in a sequence? How do humans explore the seemingly infinite space of possibilities in search of novelties? Interestingly, an insightful answer comes from biology, when, in 1996, Stuart Kauffman introduced the concept of the *adjacent possible*²⁴ (AP)—“all those molecular species that are not members of the actual, but are one reaction step away from the actual”. Inspired by previous works by Packard and Langton^{25–27}, the AP provides a fresh view on the problem, for which discoveries (the possible) can

only be found among those items which are close (the adjacent) to what is already known (the actual). New discoveries would then generate an expanding space of opportunities that are only available to us in the moment we “unlock” what is adjacent to them. Kauffman’s AP has seen many interesting applications ranging from biology^{24,28} and economics^{9,29} to models of discovery and innovation processes. Among these, of particular interest is the recently proposed Urn Model with Triggering (UMT)^{1,6,30}. Building upon the work of Pólya^{31,32}, the UMT adds to the traditional *reinforcement* mechanism of the Pólya urn’s scheme a *triggering* mechanism that expands the space of possible discoveries upon the extraction of each novelty. Being able to reproduce the empirical laws, the UMT has been used to study the rise and fall of popularity in technological and artistic productions², the emergence and evolution of social networks³³, and the evolution of the cryptocurrency ecosystem³⁴. The AP accounts for the emergence of the new starting from the “edge of what is known”. In this view, one could also picture ideas, concepts, or items as the linked elements of an abstract network. Within this framework, the way we explore the world based on the association of different concepts can be modelled as a random walk over this network. Approaches based on random walks have been used to investigate the cognitive growth of knowledge in scientific disciplines³, and further extended to account for multi-agent systems, where the individual exploration of the agent is enriched by social interactions^{14,35}.

The idea of the adjacent possible, which can be modelled either in terms of extractions from urns or random walks over a network, is of great importance to understand the processes leading to innovation. There is, however, another important mechanism of creation of the new which is neglected by the frameworks discussed above: novelties can arise from the combination of already-known elements. For instance, a meaningless sequence of words, if ordered in a different way, may generate elegant poetry. Novel combinations of existing hashtags may lead to new social-media trends. Different orderings of the same musical notes may in principle generate an endless number of songs. The mechanics of combination and association of “pre-existing” items has been studied in various fields, e.g. in biology, where combinations are the keys to produce new entities and organisms. For instance, it has been shown that the immune system recombines existing segments of genes to produce new receptors^{36,37}. Publications and collaborations in science³⁸ are typically combinations of research ideas^{39–41} and expertises^{42–44}. Similarly, in innovation economics, as originally discussed by Schumpeter^{45,46} and confirmed by recent works on the generation of technologies^{47–49}, new associations of existing factors may give rise to innovations, which rule out of the market obsolete products and services^{50,51}, thus increasing the probability of reaching further novelties and innovation (the so-called “creative destruction”).

The aim of this paper is to explore a more general notion of novelty defined as the novel combinations of existing el-

ements. We thus investigate the dynamics of “higher-order” novelties, i.e., novel combinations of pairs, triplets, etc., of consecutive items in a sequence. In particular, we focus on the Heaps’ law, which describes the growth in the number of novelties as a power-law, whose exponent is a proxy for the rate of discovery¹⁶ in a system. Namely, we introduce higher-order Heaps’ laws to characterize the rate at which novel combinations of two and more elements appear in a sequence. We then analyse various types of empirical sequences ranging from music listening records, to words in texts, and concepts in scientific articles, finding that Heaps’ laws also holds at higher orders. We discover that individual processes with the same rate of discovery of single items, can instead display different rates of discovery at higher orders, and can hence be differentiated in this way. We therefore propose a new model which is capable of reproducing all these empirically observed features of higher-order Heaps’ laws. In our model the process of exploration is described as an edge-reinforced random walks with triggering (ERRWT). In our framework, the novelties at different orders (nodes and links visited for the first time by the walker) shape the explored network by reinforcing traversed links while, at the same time, triggering the expansion of the adjacent possible. This expansion can happen whenever a node is visited for the first time, making other nodes accessible to the explorer, but also whenever a link is firstly used. In this case, the newly established connection will trigger novel combinations between previously explored nodes. By fitting the contributions of the two mechanisms of reinforcement and triggering, the ERRWT model is able to reproduce well the variety of scaling exponents found in real systems for the Heaps’ laws at different orders.

Results

Higher-order Heaps’ laws

An exploration process can be represented as an ordered set of T symbols $\mathcal{S} = \{a_1, a_2, \dots, a_T\}$. Such a set describes the sequence of “events” or “items” produced along the journey, e.g. the songs listened by a given individual over time, the list of hashtags posted on an online social network, the list of words in a text, or any other ordered list of items or ideas generated by single individuals or social groups^{1,13,35,52}. Similarly, in the context of some recent modelling schemes of discovery, \mathcal{S} can represent the balls extracted from an urn^{1,35,52}, or the nodes visited over time by a random walker moving over a network³. Although real-world events have an associated time, here, for simplicity, we focus only on their sequence, i.e. the relative temporal order of the events, neglecting the precise time at which they happen. For instance, if a person listens to song a_1 at time t_1 , song a_2 at time t_2 , song a_i at time t_i , and so on, with $t_1 < t_2 < \dots < t_i < \dots$, we neglect these times and only retain the order of the songs in the sequence $\{a_1, a_2, \dots, a_T\}$. In other words, we assume that a_1 is associated to the discrete time $t = 1$, a_2 is associated to time $t = 2$, and so forth.

Among the different ways to characterize the discovery rate

of a given process, the Heaps' law, $D(t) \sim t^\beta$, describes the power-law growth of the number of novelties as a function of time, i.e., how the number $D(t)$ of novel elements in the sequence \mathcal{S} scale with the sequence length t ¹⁶. The so-called (standard) Heaps' exponent β , that from now on we indicate as 1st-order Heaps' exponent β_1 , is thus a measure of the pace of discovery of the process that generated the considered sequence. Given that the number of different elements $D(t)$ is smaller (or equal) than the total length t of the sequence, the value of β_1 is always bounded in the interval $[0, 1]$, with the extreme case $\beta_1 = 1$ reached by a process that generates new elements at a linear rate.

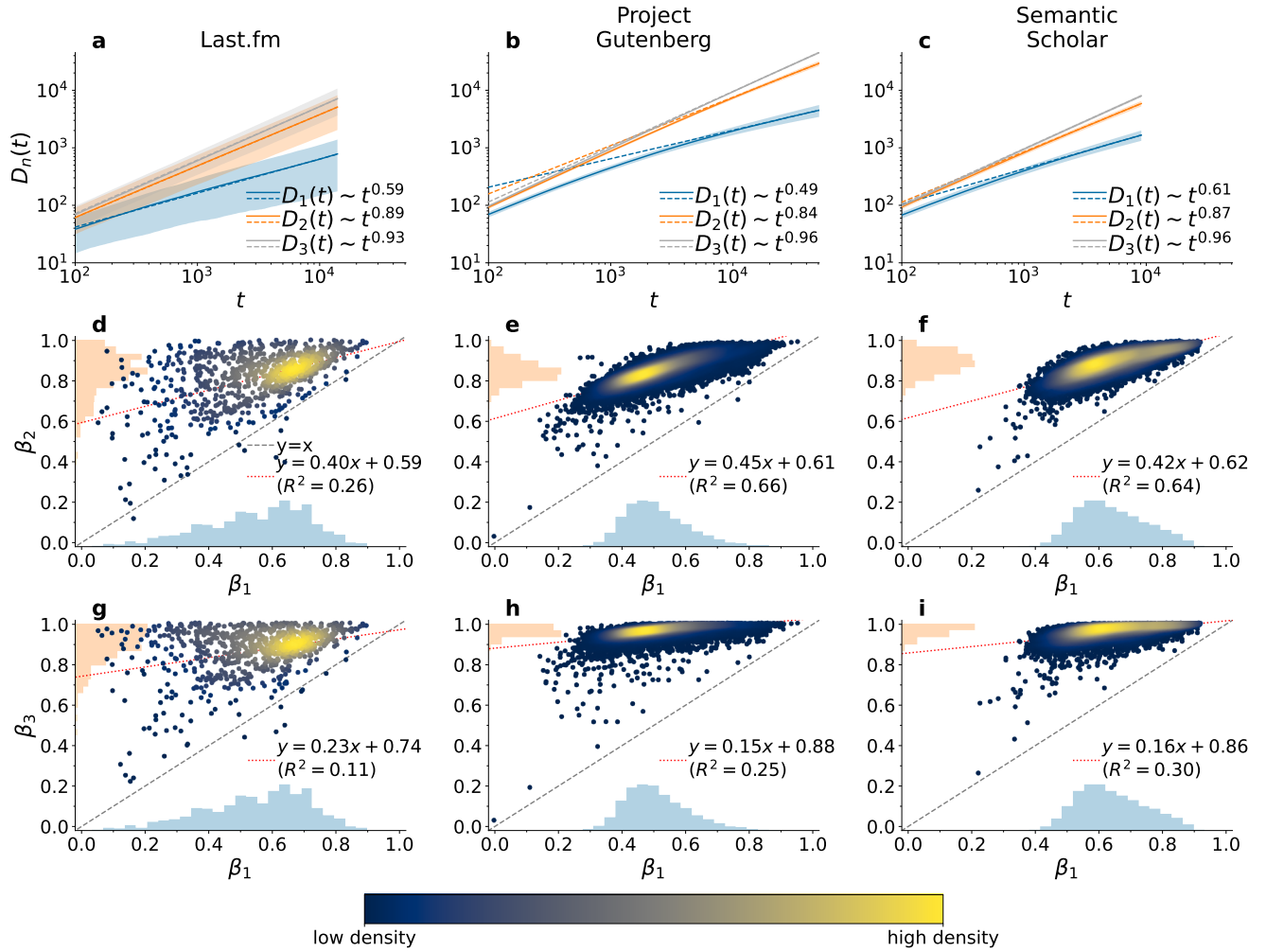
Here, we propose to go one step beyond and look at novelties as novel pairs, triples, and higher-order combinations of consecutive symbols in a sequence⁵³. For instance, when exploring a network, a novel pair is represented by the first visit of a link. In order to measure the pace of discovery of these higher-order compounds starting from a sequence of events \mathcal{S} , we first create the surrogate sequence of overlapping pairs $\mathcal{S}_2 = \{(a_1, a_2), (a_2, a_3), \dots, (a_{T-1}, a_T)\}$. Considering for example the sentence “One ring to rule them all”, from the sequence of events $\mathcal{S} = \{\text{one, ring, to, rule, them, all}\}$ we obtain the sequence of overlapping pairs $\mathcal{S}_2 = \{(\text{one, ring}), (\text{ring, to}), (\text{to, rule}), (\text{rule, them}), (\text{them, all})\}$. From \mathcal{S}_2 we can then compute the number $D_2(t)$ of different pairs among the first t ones, with $t \leq T - 1$. Notice that, in this manuscript, we consider the pairs (one, ring) and (ring, one) as two different pairs, i.e., order matters. By construction, we always have $D_1(t) \leq D_2(t) \leq t$, since, on the one hand, for each new element added to \mathcal{S} there is a new pair in \mathcal{S}_2 , and, on the other hand, there cannot be more than t different pairs among t items. From the power-law scaling $D_2(t) \sim t^{\beta_2}$, we can then extract the value of β_2 , which we refer to as the 2nd-order Heaps' exponent. This definition can be naturally extended to any order n , considering the sequence \mathcal{S}_n of consecutive overlapping n -tuples present in \mathcal{S} . Notice that, if $|\mathcal{S}| = T$, then $|\mathcal{S}_n| = T - n + 1$. We can hence compute the number $D_n(t)$ of different tuples among the first t tuples in \mathcal{S}_n , and extract the n^{th} -order Heaps' exponent $\beta_n \in [0, 1]$ from $D_n(t) \sim t^{\beta_n}$. Notice also that the n^{th} -order Heaps' exponent can be also interpreted as the first order Heaps' exponent of a sequence whose events are the overlapping n -tuples of the original sequence. Finally, it is worth remarking that such an approach is close to the analysis of Zipf's law in linguistic data for n -grams or sentences^{54,55}. In this context, studies showed that as one moves from graphemes, to words, sentences, and n -grams, the Zipf's exponent (reciprocal of the Zipf's for infinitely long sequences¹⁷) gradually diminishes. This implies that n -grams or sentences are characterized by a larger novelty rate than words, a behavior analogous to what we have discussed above.

Analysis of real-world data sequences

We start investigating the emergence of novelties of different orders in empirical exploration processes associated to three

different data sets. These data sets are substantially different in nature, since they refer, respectively, to songs listened by users of *Last.fm*, words in books collected in the *Project Gutenberg*, and words of titles of scientific journals from *Semantic Scholar* (more details on the data can be found in *Materials and Methods*). In Fig. 1(a-c) we plot the average temporal evolution of the number $D_n(t)$ of novelties of order n , with $n = 1, 2, 3$, in the three datasets (from left to right, respectively, Last.fm, Project Gutenberg, Semantic Scholar). In order to avoid spurious effects due to different lengths of the sequences, we restrict the averages to the sequences of length T greater than the median length \tilde{T} in the corresponding data set (see Fig. S1 in the Supplementary Information (SI) for their distribution). Each continuous curve, plotted up to time \tilde{T} , is obtained by averaging $D_n(t)$ over all such sequences, while the shaded area represents one standard deviation above and below the mean. We also perform power-law fits (see *Materials and Methods* for details on the procedure), and plot the resulting curves as dashed lines. Focusing first on the broadly-studied (1st-order) Heaps' law, notice how the power-law fit is only accurate in the last part of the sequence. This highlights that the Heaps' law starts after a transient phase, where most of the events are new for the individual, as also reported in Ref.¹ and similarly reported in other contexts⁵⁶⁻⁶⁰. Secondly, notice how the n^{th} -order Heaps' law, with $n = 2, 3$, is valid across the data sets, but with different values of the fitted exponents, especially for $n = 2$. Finally, as expected from their definition, the fitted Heaps' exponents of order $n + 1$, i.e., β_{n+1} , are higher than the lower-order ones, that is, $\beta_{n+1} \geq \beta_n$.

To explore the gain in information brought by the higher-order Heaps' exponents with respect to the 1st-order Heaps', we now look directly at individual sequences. Figure 1(d-i) shows the scatter plots of β_2 (d-f) and β_3 (g-i) against β_1 , where each point refers to a single sequence from Last.fm (d,g), Project Gutenberg (e,h) or Semantic Scholar (f,i), with colors representing the density of points (see color bar at the bottom of the figure). Here, we have only considered sequences whose fitted exponent has a standard error below the 0.05 threshold (see Table S1 in SI for more details). This filtering removes 30 (3.37%), 8 (0.04%), and 5 (0.03%) sequences in the three datasets, respectively. This shows that, in almost all cases, we can consider the Heaps' law assumption to be valid. Looking at the plots, we notice that some cases have a higher density of points compared to others. For example, in (d), we see how users of Last.fm sharing the same value of β_1 can have very different values of β_2 . Conversely, the other two data sets present stronger correlation between β_2 and β_1 . To quantitatively characterize this, we fit a linear model with an ordinary least squares method, displayed in each plot as a red dotted line. In the legend we also report the value of the related coefficient of determination R^2 , which represents the percentage of variance of the dependent variable explained by the linear fit with the independent variable. For users of Last.fm, at both orders $n = 2$ and 3, we quantitatively confirm



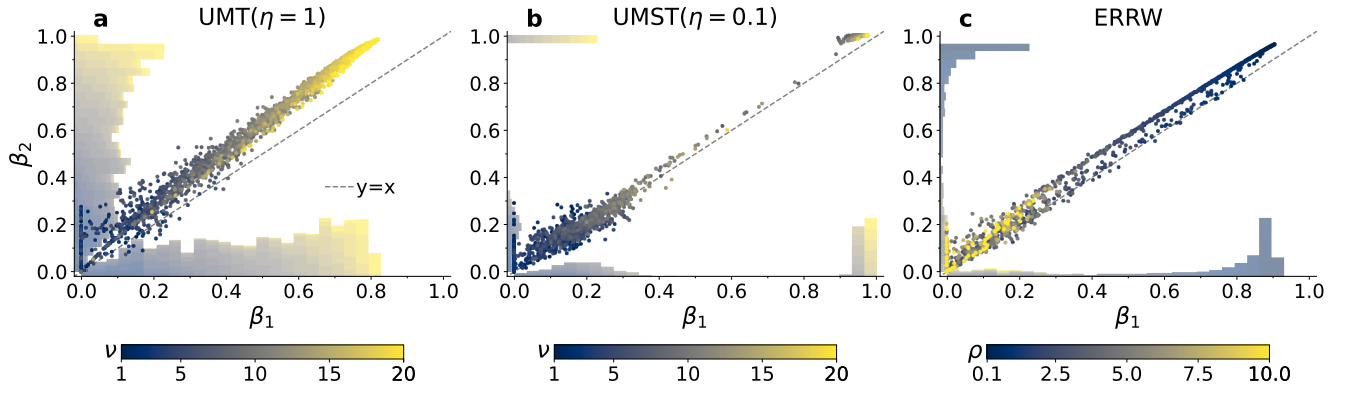


Figure 2. Higher-order Heaps' exponents in existing models. Scatter plots between the (1st-order) Heaps' exponent β_1 and the 2nd-order exponent β_2 in: (a) the urn model with triggering (UMT), no semantic correlations ($\eta = 1$), and $\rho = 20$, $v = 1, 2, \dots, 20$; (b) the urn model with semantic triggering (UMST) with $\eta = 0.1$ and $\rho = 4$, $v = 1, 2, \dots, 20$; (c) the edge-reinforced random walk (ERRW) on a small-world network (average degree $\langle k \rangle = 4$ and rewiring probability $p = 0.1$) with edge reinforcement ρ ranging geometrically from 0.1 to 10. Each point refers to a different simulation of the related model, with colors representing the value of the free parameter (see color bar). Each panel also reports histograms of exponent distributions on the respective axes, and the bisector $y = x$ (dashed gray line). All simulations have run for 10^5 time steps.

that points are much more spread around the linear fit, since the values of R^2 are very low, between 0.11 and 0.16. In the other two data sets there is instead a higher correlation between β_1 and both β_2 (R^2 around 0.70) and β_3 (R^2 around 0.35). Moreover, the values of the parameters of the linear fit greatly change across datasets and orders. In particular, in (d) there is a much lower slope and higher intercept compared to the other data sets for the same order in (e-f). Furthermore, we notice how, for each data set, the higher the order, the lower the fitted slope —and the higher the intercept of the linear model. Finally, on an aggregate level, we observe that at all orders the distribution of the Heaps' exponents are very different across data sets (see Fig. S2 in SI for a comparative figure, while further statistical information on the Heaps' exponents distribution can be found in Table S2 in SI.). The exponents are more spread in Last.fm, which also shows a higher average of β_1 and β_2 , but a lower one for β_3 compared to the other data sets. Distributions for Project Gutenberg and Semantic Scholar, which are both related to linguistic data, are more peaked —at higher values for the latter dataset. This could be the result of how titles of scientific papers are written with respect to books or poems, that is, concentrating the whole message of a scientific work in a few significant words, avoiding stop-words and repetition. In addition, scientific advancements tend to favor the combinations of previously existing scientific concepts to form new ones, while the same does not apply to non-scientific literature in general, where instead similar constructions tend to be repeated across the piece. Finally, similar results are obtained also for more coarse-grained sequences generated using artists and stemmed words instead of songs and words (see Fig S3 in SI).

Analysis of existing models

After studying higher-order Heaps' laws in real data, we check whether the observed patterns can be also reproduced by the available models for discovery processes. We start from the Urn Model with Triggering (UMT), where a sequence of events is generated by draws of coloured balls from an urn¹, different colours corresponding to different events/items being discovered/adopted and so on. In the UMT, for each extracted ball, the corresponding color is reinforced by adding ρ additional balls, of the same color, to the urn. At the same time, whenever a novel color is drawn, the discovery triggers the addition of $v + 1$ balls of new different colors to the urn (see detailed model definition in *Materials and Methods*). Previous studies have shown that the 1st-order Heaps' law is verified in sequences obtained with the UMT^{1,6}. In particular, the number of novelties in the model grows asymptotically as $D_1(t) \sim t^{\frac{v}{\rho}}$ when $v < \rho$, while a linear behaviour is found in the other cases. We hence focus on the most interesting case, that is for $v \leq \rho$, studying how variations of the two parameters ρ and v , respectively representing the reinforcement and the increase in size of the adjacent possible, affect the Heaps' law at various orders. Since the pace of discovery effectively depends only on the fraction v/ρ , we fix $\rho = 20$ and numerically simulate the UMT with $v = 1, 2, 3, \dots, 20$ for $T = 10^5$ time-steps. For each set of parameters we run 100 simulations, generating a total of 2×10^3 synthetic sequences. Then, for each generated sequence, we compute the temporal evolution of the number of novelties $D_n(t)$, and estimate a power-law fit, extracting the related n^{th} -order Heaps' exponent β_n . In Fig. 2(a), we show how the extracted values of β_2 change with respect to β_1 across simulations. The color represents the value of the parameter v , as shown in the color

bar. We observe that, although the exponents are distributed all across the interval $(0, 1)$, the points (β_1, β_2) are just above the bisector (gray dashed line). Moreover, for a certain value of β_1 , the model produces very similar values of β_2 that do not vary much. We can derive an analytical approximation of the higher-order Heaps' exponents for this model. As we show in Sec. S3.2 of the SI, for the UMT the number of unique pairs grows as

$$D_2(t) \approx at^{\beta_2}, \quad \text{with} \quad \beta_2 = \beta_1 + \frac{c}{d + \log(t)}, \quad (1)$$

where $a, c, d > 0$ depend on the parameters ρ and v , and $\beta_1 = v/\rho$. Although the predicted 2nd-order exponent is slightly higher than the 1st-order one, their difference just depends on the sequence length, and vanishes at larger times. In other words, the increased value of the higher-order Heaps' exponent is only due to a finite time effect, and the UMT struggles in reproducing the empirical patterns discussed in Fig. 1.

We repeat the analysis for the Urn Model with Semantic Triggering (UMST)¹ and the Edge-Reinforced Random Walk (ERRW)³, which have also been proved to generate discovery sequences obeying to the Heaps' law. These models share the same foundations of the UMT, but with some crucial differences. The UMST builds on top of the UMT introducing also semantic groups for colors (topic common to different items). This addition effectively diminishes the probability to draw colors outside of the semantic group of the last extracted color by a factor η . The ERRW is formulated as a network exploration rather than a process of extractions from an urn. Instead of a sequence of extracted balls, the ERRW features a set of nodes sequentially visited by a random walker over a weighted networks, where the weight of visited edges are reinforced at each time by ρ . A full description of the models can be found in *Materials and Methods*.

We simulate the UMST with parameters $\eta = 0.1$, $\rho = 4$, $v = 1, 2, \dots, 20$, while the ERRW runs over a small-world network (with average degree $\langle k \rangle = 4$ and rewiring probability $p = 0.1$), with edge-reinforcement ρ ranging from 0.1 to 10. Similarly to the exploration of the UMT, we perform 100 simulations for each set of parameters and report the results in Fig. 2(b-c). For both UMST and ERRW, we find that the values of β_2 do not differ much from their corresponding value of β_1 —as shown by the great proximity of the points (β_1, β_2) to the bisector. This means that also these models fail to reproduce the empirical variability of higher-order Heaps' exponents with respect to the 1st-order one. Moreover, we notice in (b) that for the UMST we only obtain exponents with either very low (up to 0.4) or very high (close to 1) values. It seems thus that there is an abrupt transition between the two cases, with the model not able to cover the values in-between. This is instead a crucial point when we are confronted with the empirical values reported in Fig. 1 (see also the relation with analytical results in Fig. S4 in SI).

Overall, with the analyses above we have just shown that

while the existing models for discovery and innovation dynamics are able to reproduce the empirically observed pace of discovery of new items—as singletons—they systematically fail when it comes to capturing the distributions of the Heaps' exponents of higher order and their correlations.

A model for higher-order Heaps' laws

We now introduce a model that generates synthetic sequences displaying different Heaps' exponents at various orders.

As for the previously discussed ERRW, our novel model is formulated using a network framework in which: (i) the items to be explored correspond to the nodes of the network; (ii) links between nodes represent semantic associations between items that one can use to move from one to another; (iii) the exploration process is modelled as a random walk over the network, and the exploration sequence is given by the list of visited nodes.

Under these assumptions, the first visit of a node corresponds to a 1st-order novelty, while a 2nd-order novelty refers to the first exploration of a link. This definition can be trivially extended to higher orders, but in this manuscript, for simplicity, we limit our attention to the first two orders. The ERRW proposed in Ref.³ consists of a walker exploring a static network with a fixed topology, whose movements modify only the weights of the links. By contrast, in our model the network structure (not just the weights) co-evolves over time together with the exploration process such that new links can be triggered. Thus, blending together the ERRW and the UMT¹, we call the model *Edge-Reinforced Random Walk with Triggering* (ERRWT). More specifically, the model is based on two different triggering mechanisms that add new edges and new nodes every time a novelty appears. As per the UMT and the ERRW, exploring a node for the first time triggers the expansion of the adjacent possible, as new nodes become now accessible. For example, the invention of the transistor made it possible to create mobile phones, among other things. Concerning the triggering of new edges, the idea is that whenever two elements are associated for the first time, new possible combinations involving one of these elements are then triggered. For instance, once a camera and a mobile phone were firstly combined, this made clear that many more functions could be added to the latter, e.g., a music player, a game console, a GPS, etc.

The basic mechanisms of the ERRWT model are illustrated in Fig. 3. Suppose that, at a given time t , the walker is at node i of a network composed of some already visited nodes and links (filled nodes and continuous lines), and some others that belong to the adjacent possible (unfilled nodes and dashed lines). This is the starting point of Fig. 3(a). In Fig. 3(b), the walker crosses an already explored link, and its weight gets reinforced by a term ρ , meaning that the association of the two nodes becomes more likely. This is the same reinforcement process of the ERRW in Ref.³. If addition, if the edge is instead traversed for the first time, along with the edge-reinforcement the process triggers also the creation of

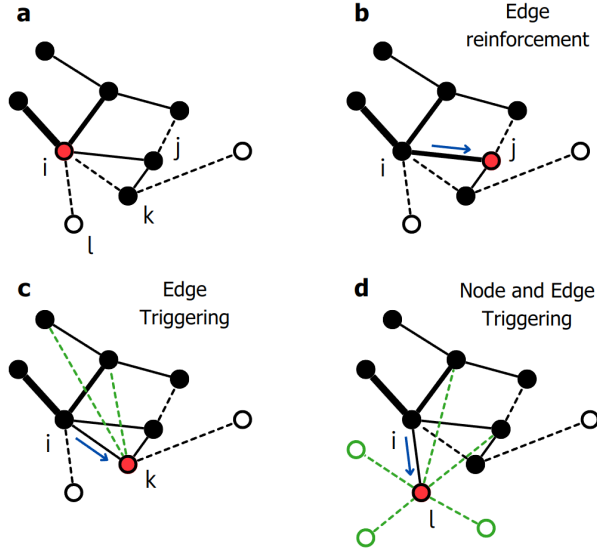


Figure 3. The Edge-Reinforced Random Walk with Triggering (ERRWT) model. An exploration process is modelled as a random walk on a growing weighted network. (a) At time t , the walker is at the red node i . Nodes that have been already visited by the walker are colored in black, in white those left to be visited. Similarly, traversed (old) and not-traversed (new) links are respectively depicted with continuous and dashed lines, whose widths represent their weights. At time $t + 1$, the walker can move to each of the neighbours of i , e.g. j , k , or l , with a probability proportional to the weight of the respective link. (b) If the walker moves to j , since the link (i, j) is old, its weight is reinforced by ρ (edge reinforcement); (c) if it moves to k , since link (i, k) is new, but node k is old, in addition to the edge reinforcement, $v_2 + 1 = 2$ new edges (in green) between k and old nodes are added to the network (edge triggering); (d) if it moves to l , since both the link and the node are new, in addition to the edge reinforcement and the edge triggering, $v_1 + 1 = 3$ new nodes (in green) are added to the network and connected to l (node and edge triggering).

new edges. In particular, as displayed in Fig. 3(c), $v_2 + 1$ new edges connecting the second node of the traversed link to other already-visited nodes are created. Finally, analogously to the triggering mechanism of the UMT, whenever a node is visited for the first time, it triggers the expansion of the node's adjacent possible with $v_1 + 1$ new nodes added to the network and connected to the node itself (Fig. 3(d)). Note that this also triggers the creation of other $v_2 + 1$ new links to already known elements, since whenever a node is explored for the first time, also the link leading to it is explored for the first time. More details about the ERRWT model can be found in *Materials and Methods*.

Balancing edge reinforcement and the node and edge triggering through the parameters ρ , v_1 and v_2 , it is possible to control the pace of discovery of new nodes and edges, and consequently the exponents of the 1st-order and the 2nd-order Heaps' law associated to the sequences produced by the model. To systematically explore this, we simulate the ERRWT model with parameters $\rho = 10$, $v_1 = 0, 1, \dots, 20$, and $v_2 = 0, 1, \dots, 2v_1$, running 100 simulations for each set of parameters. Higher values of v_2 have not been considered since they produce the same exponents as those for $v_2 = 2v_1$. Fig. 4(a) reports the increase in the number of 1st-order and 2nd-order novelties (continuous lines). The power-law fits (dashed lines) highlight that the Heaps' law is verified at higher-orders too, leading to an increase of the exponents values (from $\beta_1 = 0.56$ to $\beta_2 = 0.87$) as we increase the order. The relationship between the different orders is explored in Fig. 4(b), where we show the scatter plot between the 1st- and 2nd-order Heaps' exponent. Each point refers to a different simulation, and we use the color to indicate the value of the used parameter v_1 (see color bar). We notice that the ERRWT model produces a wide range of exponents at both orders, which are no more trivially correlated as for previous models. This is even more clear when we look at Fig. 4(c), where Heaps' exponents are averaged across simulations for each set of parameters: each trajectory relates to a different value of v_1 , with v_1 increasing from 1 to 20 from bottom left to top right of the panel. The color represents instead the variation of the parameter v_2 from 0 to $2v_1$. For reference, we also flag using a red dot the pair of exponents related to the parameters used in Fig. 4(a). We can immediately notice how the 1st- and 2nd-order Heaps' exponents increase as v_1 becomes larger. More interestingly, we can investigate the interplay with v_2 : given a single trajectory, by increasing v_2 the difference between β_1 and β_2 becomes larger, and the point (β_1, β_2) moves away from the bisector—in a way that depends on the specific value of v_1 . In particular, for low values of v_1 , the trajectories are almost vertical, with only β_2 increasing. Instead, for higher values of v_1 , especially when $v_1 \geq \rho$, an increase of v_2 produces a decrease of β_1 , while the value of β_2 , which is close to its upper bound value 1, does not change.

It is also possible to perform an analytical investigation of a simplified version of the ERRWT model, which leads to re-

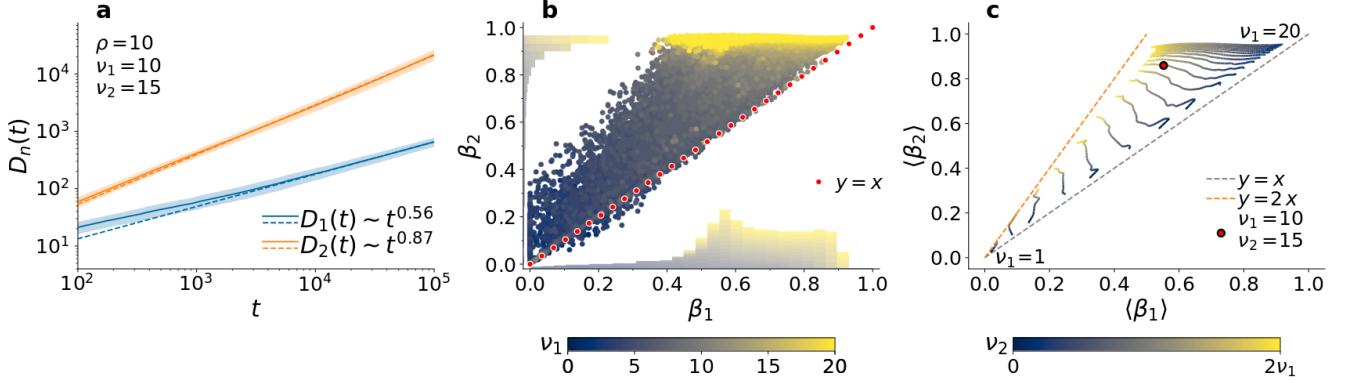


Figure 4. Higher-order Heaps' exponents in the ERRWT model. (a) Average number $D_n(t)$ of novelties of order n , with $n = 1$ and 2 , as a function of the sequence length t for simulations of the ERRWT model with parameters $\rho = 10$, $v_1 = 10$, $v_2 = 15$, and fit of the associated Heaps' laws (dashed lines), with estimated exponents shown in the legend. Shaded areas represent one standard deviation above and below the average. (b) Scatter plot between the (standard) Heaps' exponent β_1 and the 2nd-order exponent β_2 . Each point refers to a different simulation of the model, with colors representing the corresponding value of the parameter v_1 ranging from 0 to 20 (see color bar), while $\rho = 10$ and $v_2 = 0, \dots, 2v_1$. (c) Variation of the average n th-order Heaps' exponents β_n , with $n = 1, 2$. Each trajectory refers to a different value of v_1 , increasing from 1 to 20 from bottom left to top right, with the color depending on the value of v_2 (see color bar). The set of parameters used in (a) is here highlighted in with a red dot.

sults which are in agreement (see Sec. S4 in SI). In particular, for such a model, we can prove that the values of the asymptotic Heaps' exponents β_1 and β_2 depend on the two ratios v_1/ρ and v_2/ρ . Moreover, we find that, for $v_1/\rho > 1$, the 2nd-order Heaps' exponent is asymptotically equal to 1 , while the 1st-order one depends on v_1/v_2 , in agreement with our numerical results. Finally, the exponents are asymptotically bounded by $\beta_1 \leq \beta_2 \leq 2\beta_1$, as also shown in the simulations in Fig. 4(c). This also explains why the exponents do not change when we increase v_2 above $2v_1$.

Comparison between ERRWT and real-world data

To show that the ERRWT model is able to reproduce the properties observed in real-world processes, we now fit it to the three data sets analyzed (Last.fm, Project Gutenberg and Semantic Scholar). Given an empirical sequence and its pair of 1st- and 2nd-order Heaps exponents (β_1, β_2) , we compute the Euclidean distance between the pair (β_1, β_2) and each of the pairs of exponents (β'_1, β'_2) obtained by simulating the ERRWT model using the sets of parameters considered in the previous section. We then select the best model parameters by minimizing the average distance over 100 simulations for each set, and repeat the procedure for all the sequences of the three data sets. Figure 5(a) shows the probability density distribution of the distances between the empirical sequences and the simulations of the best-performing ERRWT model. Notice how these distances are almost all below 0.1 , that is to the uncertainty we expect on the values of the parameters. In fact, being v_1, v_2 integers and $\rho = 10$, the maximum precision we can gain on the estimate of the best parameters is $1/\rho = 0.1$. The percentage of sequences with higher distance than

this threshold is 7.67%, 0.73%, and 0.05% for Last.fm, Project Gutenberg, and Semantic Scholar, respectively. The scatter plots of the best-fitted parameters v_1 and v_2 for the three data sets are shown in Fig. 5(b-d). The colors here indicate the number of empirical sequences which are best represented by each pair of parameters. We notice that most of the sequences of Last.fm are characterized by relatively large values of v_1 . Since v_1 is related to the triggering of new nodes, this result indicates that the discovery of a new song exposes the user to a large variety of related songs, which were previously not accessible and can now be discovered. Conversely, the parameter v_2 , which refers to the triggering of new edges between already existing items, takes values in a larger range, predominantly skewed towards the lower end. This suggests that, once a new association of two songs is established by a user, there is a high probability that the same association will be repeated over and over. Consequently, the user will preferably listen to songs in a similar order, instead of creating new associations. In the case of Project Gutenberg, most sequences have $v_2 > v_1$. This implies that writers tend to frequently generate new word associations, highlighting the incredible variety of expressions we can make combining a limited set of words. Finally, Semantic Scholar exhibits values of v_1 and v_2 similar to Project Gutenberg. However, some sequences of Semantic Scholar have a relatively high value of v_1 with respect to v_2 . This is an indication that, when choosing words for titles, authors tend to use more original words, while the pace of creation of new word associations remains similar.

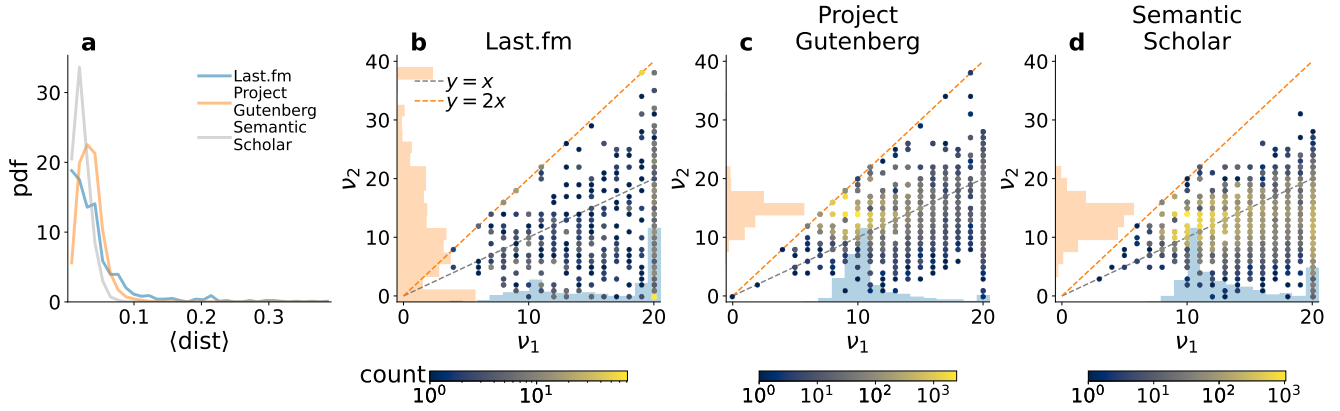


Figure 5. Fitting the ERRWT model to real-world data sets. (a) Distribution of the average distance between the pair of exponents (β_1, β_2) of a real sequence and the pair (β'_1, β'_2) obtained by the best fit of the ERRWT model. (b-c) Scatter plots of the best-fitted parameters ν_1 and ν_2 of the model across the sequences of the three data sets, i.e., Last.fm (b), Project Gutenberg (c), and Semantic Scholar (d). The color of a point refers to the number of sequences with that pair of parameters as corresponding best fit (see color bar).

Discussion

The ubiquitous appearance of the Heaps' law in various contexts has recently allowed the measurement of the pace at which discoveries occur^{1-3,61,62}. However, there is more and more evidence that discoveries are often made from the combination of different elements together^{39,41,42,48,49}. In this manuscript we have hence introduced the higher-order Heaps' exponents as a measure for the pace of new combinations realised in a system. In particular, we regard a novelty not only as the discovery of new items, but also as the first appearance of a new combination of two or more items. Notice how this measure differs from other measures for the pace of discovery that have been developed in the last years. For example, in Refs.^{8,63}, the authors have used the number of all possible valid combinations that can be created using the elements so far acquired as a proxy of the level of innovation reached by the system. However, this does not take into account the actual number of novelties realised in the system and their pace of discovery, but rather their potential.

As we have seen in empirical data, higher-order Heaps' exponents can be used to distinguish users listening to music in Last.fm who feature a similar discovery rate of new songs and artists. The higher-order Heaps' exponent can indeed tell apart different ways to explore the same set of songs in terms of number of different consecutive pairs or higher-order structures explored. Analogously, we notice different patterns in texts of various nature by studying their Heaps' exponents at multiple orders: titles of peer-reviewed papers published in scientific journals show more creative juxtaposition of words with respect to the text of narrative books, encountering many more new n -grams, even if the total set of words used is similar in length. Overall, our analysis shows that the space of possibilities grows in more complex ways, which does not

depend solely on the balance between old items to exploit and new ones to explore, but also on the structure of their associations.

We have hence focused our attention in understanding the underlying mechanisms at the core of such differences in the pace of discovery of higher-order novelties. In particular, we have extracted higher-order Heaps' exponents from synthetic sequences generated through existing models of discovery and exploration, from the urn model with triggering¹ to the edge-reinforced random walk³. On the one hand, these models are able to reproduce different behaviors in terms of 1st-order Heaps' exponents. On the other hand, however, we find that they are not able to reproduce higher-order ones. This analysis manifests the need for a new generation of exploit-vs-explore models based on the co-evolution of the network structure with the dynamical process of exploration. We have thus proposed a new modelling framework, the Edge-Reinforced Random Walk with Triggering, which takes into account not only the exploration rate of new items, but also the predisposition to explore the same content in a more creative way. Based on the reinforcement of exploited links of a complex network and the triggering of new nodes and links whenever new parts of the adjacent possible space are explored, these mechanisms give a new intuition of how the space of possibilities grows over time, shedding light on how novel elements and combinations emerge along the process.

We acknowledge there are multiple venues of improvement of the modelling scheme we have proposed. For example, future work should investigate the interplay between initial knowledge, either of the individual or of the society, and the pace of discovery at various orders during the exploration process. In our model, we have supposed that links start with unitary weight, but this can be an unrealistic assumption in certain contexts. Moreover, we have assumed to trigger new

links uniformly at random. It would be interesting to study cases in which the space has some preferential pathways, for example represented by an underlying structure that can be discovered. This could be implemented in our model by limiting the addition of new links to only those permitted by the underlying network, or adding more complex ways to trigger edges, e.g., using preferential attachment^{64,65}.

Finally, in this manuscript we have not considered the presence of semantic correlations in the temporal sequence of visited items, which can be a consequence of the interplay between the network topology and a predisposition to move within items semantically close to the recent ones, reinforcing a clustered structure. It would indeed be interesting to use higher-order Heaps' exponents and the ERRWT model to study phenomena related to waves of novelties² and popularity⁶⁶. Moreover, the ERRWT model could be extended to a multi-agent model to study how different agents would co-operate and diffuse knowledge^{14,35}, also taking into account the presence of a limited attention capacity and memory that could influence the rise and fall of popular items⁶⁷. We believe that our model can be directly used to answer these questions and, more in general, to better understand the fundamental mechanism behind innovation and creativity.

Materials and Methods

Data

In this work we consider three different data sets on music listening records (*Last.fm*), books (*Project Gutenberg*), and scientific articles (*Semantic Scholar*).

Last.fm is a digital platform for music born in 2002, famous for logging all listening activities of its users, providing both personal recommendations and a space to interact with other users interested in music⁶⁸. In this manuscript, we use a data set presented in Ref.⁶⁹ and available at Ref.⁷⁰. It contains all listening records of about 1000 users. In order to have sequences long enough for statistically relevant fits, only users with more than 1000 logs have been retained. The final data set contains 890 users having a median number of listened records of 13 985. Each record contains the timestamp at which a user listened to a given song. In the database, each song is associated to a title, the artist's name and a unique MusicBrainz Identifier (MBID), which can be used to obtain additional metadata⁷¹. Using this information, we are able to create, for each user, a temporally ordered sequence of songs together with the associated sequence of artists.

Project Gutenberg is an open access text corpus containing more than 50 000 books of different nature. Here, we make use of the Standardized Project Gutenberg Corpus⁷², which allows to download and process an updated version of the corpus. Using Google's Compact Language Detector 3 (cld3 package in Python), we filter out all non-English texts. We then discard all texts with less than 1000 words, retaining a total of 19 637 books with a median number of 50 726

words. A sequence of events for each book is hence created with the lemmatized words, disregarding punctuation and putting all characters in lower case. We also extract stems from each word using the English Snowball stemmer⁷³—a more accurate extension of the Porter stemmer⁷⁴—, which is not as aggressive as the Lancaster stemmer⁷⁵.

Semantic Scholar is a recent project with the scope of facilitating scientific analysis of academic publications. It provides monthly snapshots of research papers published in all fields, publicly accessible through the *Semantic Scholar Academic Graph* (S2AG, pronounced "stag")⁷⁶. This database (1st Jan. 2022 snapshot) contains about 203.6M papers, 76.4M authors, and 2B citations. It also classifies each paper into one or more fields of study⁷⁷, for a total of 19 different fields. For simplicity, we associate each paper to its first (and most relevant) field of study. To create the sequences to analyze, for each field we consider the first 1000 journals in terms of number of English papers. Then, for each journal, we order the published papers based on the respective year of publication, volume, issue, and first page. When some of this information is not available, the Semantic Scholar unique ID of the paper is also used in the ordering process. Thus, for each paper, we extract and lemmatize their title, similarly to what done for the Project Gutenberg. Finally, a sequence of events is created for each selected journal, concatenating the lemmatized words in the titles of each paper in their temporal order, for a total of 19 000 sequences with median length of 9 114.5. Associated to this sequence, we also consider the sequence of stemmed words for further analysis.

Power-law fit

Fundamental for the estimation of the higher-order Heaps' exponent of a sequence is the power-law fitting procedure for the number of novel n -tuples $D_n(t)$ as a function of the sequence length t , with $n \geq 1$. The sequences analyzed in this work come from very different contexts, from empirical data sets to model simulations. We thus need to take into consideration all those cases that show a transient regime—whose length might also depend on the system structure³⁵—in which the pace of discovery can fluctuate before reaching its stationary value. We fit each sequence according to the following procedure. To reduce computational times, we first logarithmically sample 1000 points from each sequence in the range $[1, T]$. Considering their integer part and discarding all duplicates, we obtain a set of k integer times $\{t_i\}_{i=1,\dots,k}$ between 1 and T . If $T \geq 1000$, that is the case of all sequences used in this manuscript, then this process results in $k \geq 424$ points. Taking into account that the associated sequence of n -tuples has length $T - n + 1$, we thus consider the points $\{(t_i - n + 1, D_n(t))\}_{i=1,\dots,k}$ in logarithmic scale, i.e.,

$$(x_i, y_i) = (\log_{10}(t_i - n + 1), \log_{10}(D_n(t))), \quad (2)$$

with $i = 1, \dots, k$. In order to neglect the initial transient regime, but still have enough points for a sufficiently significant fit, we

select only the last 100 of such points. We hence look for the best fit of $\{(x_i, y_i)\}_{i=k-100+1, \dots, k}$ by optimizing the linear function $y = a + bx$, with $a > 0$, using the tool `curve_fit` of the Python package `Scipy`⁷⁸. If \bar{a} and \bar{b} are the best parameters, then the power-law fit of the Heaps' law is $D_n(t) \approx 10^{\bar{a}} t^{\bar{b}}$, that is, the n^{th} -order Heaps' exponent is approximated by the slope \bar{b} of the fit.

Urn Model with (Semantic) Triggering

The Urn Model with Triggering (UMT) is a generative model of a discovery process, producing a sequence of extractions of balls of various colors, representing different events, from an urn. First introduced in Ref.¹, it successfully reproduces the main features of empirical discovery and innovation processes^{1,6,52,79}. The UMT can be thought as an extension of Pólya Urn processes^{31,32,80–82} that includes the concept of *adjacent possible*²⁴ in the way a novelty can trigger further ones^{2,30}. Differently from the classic urn of Pólya in which only balls of existing colors can be added to the urn, the UMT features a growing number of colors, that is, the set of possible events expands together with the exploration process. It is hence the process itself that shapes the content of the urn by reinforcing elements already discovered and adding new possibilities.

Supposing that the urn initially contains N_0 balls of different colors, the UMT works as follows. At each discrete time-step t , a ball is randomly drawn from the urn with uniform probability, and its color is marked in a temporally-ordered sequence of events \mathcal{S} at position t . The extracted ball is then put back in the urn together with other ρ copies of the same color, in a *rich-get-richer* manner⁶⁴. This mechanism ensures that frequently adopted items, visited places, or exploited concepts will be more and more likely to be adopted, visited, or exploited in the future. Furthermore, if the color of the extracted ball has never appeared before in \mathcal{S} , this event is considered to be a novelty. As a consequence it triggers new possibilities, represented by the addition of $v + 1$ balls—each of a new different color—into the urn. This triggering mechanism thus ensures the expansion of the space of possibilities.

In a different version of the model, the Urn Model with Semantic Triggering (USMT), the sequences produced contain semantic correlations between consecutive extractions, as seen in the data¹. The UMST works similarly to the UMT, but with the introduction of semantic groups. In particular, at each triggering event, supposing that the triggering color belongs to the group A , the new $v + 1$ colors are assigned to a common new group B , semantically related to the triggering color. Therefore, a color i of label A is semantically related to all other colors of label A (siblings), the color that triggered the addition of A in the urn (parent), as well as all colors of label B that have been triggered by i (children). Taking this into consideration, at each extraction, the probability to extract each color changes depending on a fixed parameter $\eta \in [0, 1]$. A ball has weight 1 if its color is semantically related to the one extracted on the previous time-step, other-

wise it has weight η . Notice that we can recover the original UMT by simply considering $\eta = 1$. As shown in Ref.¹, the effect of N_0 is negligible at large times. For simplicity, we thus consider $N_0 = 1$ in our simulations of both UMT and UMST.

Edge-Reinforced Random Walk

Given a weighted connected graph $G = (\mathcal{V}, \mathcal{E})$ with $N = |\mathcal{V}|$ nodes and $M = |\mathcal{E}|$ links, the Edge-Reinforced Random Walk (ERRW) is a dynamical process that reinforces the weights of the visited edges in \mathcal{E} , leading to Heaps' laws³. The weights of the links in the networks quantify the strength of the relationship among nodes, and are encoded in a time-varying adjacency matrix $W^t \equiv \{w_{ij}^t\}$. This matrix features non-zero entries w_{ij}^t when at time t the link connecting node i and node j is different from zero. Let us assume that at time $t = 0$ each link $(i, j) \in \mathcal{E}$ has weight $w_{ij}^0 = 1$, while all other weights are set to zero. At each time step, a walker at node i walks to a neighboring node j with a probability that is proportional to the weight of the corresponding link, i.e., $\mathbb{P}(i \rightarrow j) = w_{ij}^t / \sum_l w_{il}^t$. After moving to the chosen node j , a reinforcement ρ is added to the weight of the traversed edge (i, j) , i.e., $w_{ij}^{t+1} = w_{ij}^t + \rho$. Given an underlying structure, the ERRW can generate sequences of visited nodes associated to a different pace of discovery by tuning the reinforcement parameter³. The interplay between structure and dynamics means that different structures might require different values of the reinforcement parameter to reach the same pace of discovery (Heaps' law). For example, higher values of ρ must be chosen for a graph with a higher average degree. This is similar to what happens in the UMT, in which we need higher values of the reinforcement parameter ρ to obtain the same pace of discovery as we increase the triggering parameter v .

Edge-Reinforced Random Walk with Triggering

In this manuscript we propose a generative model of a discovery process based on the exploration of a growing network, i.e., the Edge-Reinforced Random Walk with Triggering (ERRWT), which can be considered as a UMT-inspired extension of the ERRW model. For this model, any initial connected network $G^0 = (\mathcal{V}^0, \mathcal{E}^0)$ with $N^0 = |\mathcal{V}^0| \geq 1$ nodes and $M^0 = |\mathcal{E}^0|$ links can be used. Let us suppose that the nodes of the graph are indexed, that is, $\mathcal{V}^0 = \{1, 2, \dots, N_0\}$. Similarly to the ERRW model, we assume that all initial links $(i, j) \in \mathcal{E}^0$ have weight $w_{ij}^0 = 1$. The initial node to start the exploration process is randomly selected from \mathcal{V}^0 . We let the graph evolve during the process, adding new nodes and links. Let $G^t = (\mathcal{V}^t, \mathcal{E}^t)$ be the graph at time t . The structure of the growing network is encrypted in the time-varying weighted adjacency matrix $W^t \equiv \{w_{ij}^t\}$, where w_{ij}^t represents the weight of the link (i, j) at time t . We assume here that G^t is an undirected graph, so the matrix W^t is symmetric, and any variation of w_{ij}^t affects w_{ji}^t too. Supposing that at time t the ERRWT is positioned on node i of G^t , the model obeys to the following rules.

- *Choice of next node.* The ERRWT randomly moves to a neighbouring node j of the current node i . The probability to move to node j depends on the weight of the outgoing links of i , i.e.,

$$\mathbb{P}(i \rightarrow j) = \frac{w_{ij}^t}{\sum_l w_{il}^t}. \quad (3)$$

- *Edge reinforcement.* The weight of the chosen edge (i, j) is reinforced by ρ , that is,

$$w_{ij}^{t+1} = w_{ij}^t + \rho. \quad (4)$$

- *Edge triggering.* If the walker never traversed the chosen edge (i, j) before this time, i.e., it is a new link, then $v_2 + 1$ new possible links are added to the network. These links are connections of unitary weight between j and previously visited nodes $l = l_1, \dots, l_{v_2}$ in \mathcal{V}^t , for which the link (j, l) has never been traversed by the walker. If one of these edges already exists in the space of possibilities, its weight is reinforced by one more unit, otherwise, it is added to \mathcal{E}^{t+1} . In other words, we have

$$w_{jl}^{t+1} = w_{jl}^t + 1, \quad l = l_1, \dots, l_{v_2} \mid l \text{ old}, (j, l) \text{ new}. \quad (5)$$

- *Node triggering.* If the walker never visited the chosen node j before this time, i.e., it is a new node, then $v_1 + 1$ new nodes are added to the network; these are connected to node j with unitary weights. Mathematically, we have

$$\begin{aligned} \mathcal{V}^{t+1} &= \mathcal{V}^t + \{l\}_{l=|\mathcal{V}^t|+1, \dots, |\mathcal{V}^t|+v_1+2} \\ w_{jl}^{t+1} &= 1, \quad l = |\mathcal{V}^t| + 1, \dots, |\mathcal{V}^t| + v_1 + 2. \end{aligned} \quad (6)$$

Notice that if the chosen node j is new, then also the traversed edge (i, j) is necessarily new as well. Therefore, in this case there is also a triggering of $v_2 + 1$ edges from j to other previously visited nodes, as described before.

Finally, in this manuscript, we let G_0 be a small graph that emulates the triggering mechanism introduced, shown in Fig. S8 in SI. This is a regular tree with branching parameter $v_1 + 1$ and 2 levels, where the leaves are considered new, while all other nodes have already triggered. In other words, a root node has triggered $v_1 + 1$ nodes connected to it, and again these nodes have also triggered each $v_1 + 1$ other nodes. Therefore, we initially suppose that the triggered nodes, which are $v_1 + 2$ in number, are all known to the walker at the start of the simulation, and do not trigger again when later explored. Moreover, we assume that all links are new to the walker and have unitary weight. This initialization makes sure that in the initial stages of the simulation there are enough possible links between already known nodes. As we show in Sec. S4 in SI where we test different initial graphs, the initialization procedure only affects thermalization times, and becomes irrelevant asymptotically.

Data and code availability

The data used in this manuscript is publicly available at Refs.^{70,72,76}. All the code used to download, process and analyse the data and the models can be found at Ref.⁸³.

References

1. Tria, F., Loreto, V., Servedio, V. D. P. & Strogatz, S. H. The dynamics of correlated novelties. *Scientific Reports* **4**, 1–8 (2014).
2. Monechi, B., Ruiz-Serrano, A., Tria, F. & Loreto, V. Waves of novelties in the expansion into the adjacent possible. *PLoS one* **12**, e0179303 (2017).
3. Iacopini, I., Milojević, S. & Latora, V. Network dynamics of innovation processes. *Physical Review Letters* **120**, 048301 (2018).
4. North, M. *Novelty: A history of the new* (University of Chicago Press, 2013).
5. Rzhetsky, A., Foster, J. G., Foster, I. T. & Evans, J. A. Choosing experiments to accelerate collective discovery. *Proceedings of the National Academy of Sciences U.S.A.* **112**, 14569–14574 (2015).
6. Loreto, V., Servedio, V. D. P., Strogatz, S. H. & Tria, F. Dynamics on expanding spaces: modeling the emergence of novelties. In *Creativity and universality in language*, 59–83 (Springer, 2016).
7. Puglisi, A., Baronchelli, A. & Loreto, V. Cultural route to the emergence of linguistic categories. *Proceedings of the National Academy of Sciences U.S.A.* **105**, 7936–7940 (2008).
8. Fink, T., Reeves, M., Palma, R. & Farr, R. Serendipity and strategy in rapid innovation. *Nature communications* **8**, 1–9 (2017).
9. Saracco, F., Di Clemente, R., Gabrielli, A. & Pietronero, L. From innovation to diversification: a simple competitive model. *PLoS One* **10**, e0140420 (2015).
10. Abbas, K. *et al.* Popularity and novelty dynamics in evolving networks. *Scientific Reports* **8**, 1–10 (2018).
11. Rodi, G. C., Loreto, V. & Tria, F. Search strategies of wikipedia readers. *PLoS One* **12**, e0170746 (2017).
12. Sreenivasan, S. Quantitative analysis of the evolution of novelty in cinema through crowdsourced keywords. *Scientific Reports* **3**, 1–11 (2013).
13. Iacopini, I. & Latora, V. On the dual nature of adoption processes in complex networks. *Frontiers in Physics* **9**, 604102 (2021).
14. Di Bona, G. *et al.* Social interactions affect discovery processes. *arXiv preprint arXiv:2202.05099* (2022).
15. Herdan, G. *Type-token Mathematics: A Textbook of Mathematical Linguistics*, vol. 4 (Mouton en company, 1960).
16. Heaps, H. S. *Information Retrieval: Computational and Theoretical Aspects* (Academic Press, Inc., Orlando, FL, USA, 1978).
17. Lü, L., Zhang, Z.-K. & Zhou, T. Zipf's law leads to heaps' law: Analyzing their relation in finite-size systems. *PLoS one* **5**, e14139 (2010).
18. Estoup, J.-B. *Gammes sténographiques* (Institut sténographique de France, 1916).
19. Zipf, G. K. Relative frequency as a determinant of phonetic change. *Harvard studies in classical philology* **40**, 1–95 (1929).
20. Zipf, G. K. The psychobiology of language (1935).
21. Zipf, G. K. Human behavior and the principle of least effort. cambridge, (mass.): Addison-wesley, 1949, pp. 573. *Journal of Clinical Psychology* **6**, 306–306 (1950).
22. De Marzo, G., Gabrielli, A., Zaccaria, A. & Pietronero, L. Dynamical approach to zipf's law. *Physical Review Research* **3**, 013084 (2021).
23. Taylor, L. R. Aggregation, variance and the mean. *Nature* **189**, 732–735 (1961).
24. Kauffman, S. A. Investigations: The nature of autonomous agents and the worlds they mutually create. In *SFI working papers* (Santa Fe Institute, 1996).
25. Packard, N. H. Adaptation toward the edge of chaos. *Dyn. Patterns Complex Syst.* **212**, 293 (1988).

26. Langton, C. Computation at the edge of chaos: Phase transition and emergent computation (1990).
27. Langton, C., Taylor, C., Farmer, J. & Rasmussen, S. *Artificial Life II* (Avalon Publishing, 2003).
28. Bak, P. & Sneppen, K. Punctuated equilibrium and criticality in a simple model of evolution. *Physical Review Letters* **71**, 4083 (1993).
29. Armano, G. & Javarone, M. A. The beneficial role of mobility for the emergence of innovation. *Scientific Reports* **7**, 1–8 (2017).
30. Gravino, P., Monechi, B., Servedio, V. D. P., Tria, F. & Loreto, V. Crossing the horizon: exploring the adjacent possible in a cultural system. In *Proceedings of the Seventh International Conference on Computational Creativity, Paris*. (2016).
31. Eggenberger, F. & Pólya, G. über die statistik verketteter vorgänge. *ZAMM - Journal of Applied Mathematics and Mechanics / Zeitschrift für Angewandte Mathematik und Mechanik* **3**, 279–289 (1923).
32. Hoppe, F. M. Pólya-like urns and the ewens' sampling formula. *Journal of Mathematical Biology* **20**, 91–94 (1984).
33. Ubaldi, E., Burioni, R., Loreto, V. & Tria, F. Emergence and evolution of social networks through exploration of the adjacent possible space. *Communications Physics* **4**, 1–12 (2021).
34. Marzo, G. D., Pandolfelli, F. & Servedio, V. D. P. Modeling innovation in the cryptocurrency ecosystem. *Scientific Reports* **12**, 12942 (2022).
35. Iacopini, I., Di Bona, G., Ubaldi, E., Loreto, V. & Latora, V. Interacting discovery processes on complex networks. *Physical Review Letters* **125**, 248301 (2020).
36. Market, E. & Papavasiliou, F. N. V (d) j recombination and the evolution of the adaptive immune system. *PLoS Biology* **1**, e16 (2003).
37. Jones, J. M. & Gellert, M. The taming of a transposon: V (d) j recombination and the immune system. *Immunological Reviews* **200**, 233–248 (2004).
38. Fortunato, S. *et al.* Science of science. *Science* **359** (2018).
39. Uzzi, B., Mukherjee, S., Stringer, M. & Jones, B. Atypical combinations and scientific impact. *Science* **342**, 468–472 (2013).
40. Ke, Q., Ferrara, E., Radicchi, F. & Flammini, A. Defining and identifying sleeping beauties in science. *Proceedings of the National Academy of Sciences U.S.A.* **112**, 7426–7431 (2015).
41. Wang, J., Veugelers, R. & Stephan, P. Bias against novelty in science: A cautionary tale for users of bibliometric indicators. *Research Policy* **46**, 1416–1436 (2017).
42. Fontana, M., Iori, M., Montobbio, F. & Sinatra, R. New and atypical combinations: An assessment of novelty and interdisciplinarity. *Research Policy* **49**, 104063 (2020).
43. Wu, L., Wang, D. & Evans, J. A. Large teams develop and small teams disrupt science and technology. *Nature* **566**, 378–382 (2019).
44. Alvarez-Rodriguez, U. *et al.* Evolutionary dynamics of higher-order interactions in social networks. *Nature Human Behaviour* **5**, 586–595 (2021).
45. Schumpeter, J. A. *et al.* *Business cycles*, vol. 1 (McGraw-Hill New York, 1939).
46. Schumpeter, J. A. *Capitalism, socialism and democracy* (routledge, 2013).
47. McNerney, J., Farmer, J. D., Redner, S. & Trancik, J. E. Role of design complexity in technology improvement. *Proceedings of the National Academy of Sciences U.S.A.* **108**, 9008–9013 (2011).
48. Abbasiharofteh, M., Kogler, D. F., Lengyel, B. *et al.* Atypical combination of technologies in regional co-inventor networks. *Papers in Evolutionary Economic Geography (PEEG)* **20** (2020).
49. Lambert, B. *et al.* The pace of modern culture. *Nature Human Behaviour* **4**, 352–360 (2020).
50. Jin, C., Song, C., Bjelland, J., Canright, G. & Wang, D. Emergence of scaling in complex substitutive systems. *Nature Human Behaviour* **3**, 837–846 (2019).
51. Leroi, A. M. *et al.* On revolutions. *Palgrave Communications* **6**, 1–11 (2020).
52. Tria, F., Loreto, V. & Servedio, V. D. P. Zipf's, heaps' and taylor's laws are determined by the expansion into the adjacent possible. *Entropy* **20**, 752 (2018).
53. Sinatra, R., Condorelli, D. & Latora, V. Networks of motifs from sequences of symbols. *Physical Review Letters* **105**, 178702 (2010).
54. Ha, L. Q., Hanna, P., Ming, J. & Smith, F. J. Extending zipf's law to n-grams for large corpora. *Artificial Intelligence Review* **32**, 101–113 (2009).
55. Ryland Williams, J. *et al.* Zipf's law holds for phrases, not words. *Scientific reports* **5**, 12209 (2015).
56. Csányi, G. & Szendrői, B. Structure of a large social network. *Physical Review E* **69**, 036131 (2004).
57. Glänzel, W. Characteristic scores and scales: A bibliometric analysis of subject characteristics based on long-term citation observation. *Journal of Informetrics* **1**, 92–102 (2007).
58. Milojević, S. Modes of collaboration in modern science: Beyond power laws and preferential attachment. *Journal of the american society for Information science and technology* **61**, 1410–1423 (2010).
59. Milojević, S. Power law distributions in information science: Making the case for logarithmic binning. *Journal of the American Society for Information Science and Technology* **61**, 2417–2425 (2010).
60. Gerlach, M. & Altmann, E. G. Stochastic model for the vocabulary growth in natural languages. *Physical Review X* **3**, 021006 (2013).
61. Cattuto, C., Loreto, V. & Pietronero, L. Semiotic dynamics and collaborative tagging. *Proceedings of the National Academy of Sciences* **104**, 1461–1464 (2007).
62. Cattuto, C., Baldassarri, A., Servedio, V. D. P. & Loreto, V. Vocabulary growth in collaborative tagging systems. *arXiv preprint arXiv: 0704.3316* (2007).
63. Fink, T. & Reeves, M. How much can we influence the rate of innovation? *Science Advances* **5**, eaat6107 (2019).
64. Barabási, A.-L. & Albert, R. Emergence of scaling in random networks. *Science* **286**, 509–512 (1999).
65. Bianconi, G. & Barabási, A.-L. Competition and multiscaling in evolving networks. *Europhysics letters* **54**, 436 (2001).
66. Monechi, B., Gravino, P., Servedio, V. D. P., Tria, F. & Loreto, V. Significance and popularity in music production. *Royal Society Open Science* **4**, 170433 (2017).
67. Castaldo, M., Venturini, T., Frasca, P. & Gargiulo, F. Junk news bubbles modelling the rise and fall of attention in online arenas. *new media & society* **24**, 2027–2045 (2022).
68. Last.fm. Description page. <https://www.last.fm/about> (Accessed: January 2021).
69. Celma, O. *Music Recommendation and Discovery in the Long Tail* (Springer, 2010).
70. Last.fm. Music recommendation datasets for research. last.fm dataset - 1k users. <http://ocelma.net/MusicRecommendationDataset/lastfm-1K.html> (2009). Accessed: January 2021.
71. MusicBrainz. Home page. <https://musicbrainz.org/> (2022). Accessed: June 2022.
72. Gerlach, M. & Font-Clos, F. A standardized project gutenber corpus for statistical analysis of natural language and quantitative linguistics. *Entropy* **22**, 126 (2020).
73. Porter, M. F. Snowball: A language for stemming algorithms (2001).
74. Porter, M. F. An algorithm for suffix stripping. *Program* (1980).
75. Paice, C. D. Another stemmer. *SIGIR Forum* **24**, 56–61 (1990).
76. Ammar, W. *et al.* Construction of the literature graph in semantic scholar. In *NAACL* (2018).
77. Allen Institute for AI. Semantic scholar's paper field of study classifier. https://github.com/allenai/s2_fos. Accessed June 8, 2022 (2022).
78. Virtanen, P. *et al.* Scipy 1.0: fundamental algorithms for scientific computing in python. *Nature Methods* **17**, 261–272 (2020).

79. Tria, F., Crimaldi, I., Aletti, G. & Servedio, V. D. P. Taylor's law in innovation processes. *Entropy* **22**, 573 (2020).
80. Pólya, G. Sur quelques points de la théorie des probabilités. In *Ann. Inst. Henri Poincaré*, vol. 1, 117–161 (1930).
81. Johnson, N. L. & Kotz, S. Urn models and their application; an approach to modern discrete probability theory (1977).
82. Mahmoud, H. Pólya urn models crc press. *Boca Raton FL* (2009).
83. Di Bona, G., Iacopini, I., Petralia, A. & Latora, V. Code used to download, process and analyse the data and the models at higher orders. <https://github.com/gabriele-di-bona/higher-order-heaps-laws> (2023).
84. King, T., Butcher, S. & Zalewski, L. *Apocrita - High Performance Computing Cluster for Queen Mary University of London* (2017).
85. Inc., W. R. Mathematica, Version 12. URL <https://www.wolfram.com/mathematica>. Champaign, IL, 2022.

Acknowledgements

A.P. and V.L. acknowledge support from the PNRR GRInS Project. I.I. acknowledges support from the James S. McDonnell Foundation 21st Century Science Initiative Understanding Dynamic and Multi-scale Systems - Postdoctoral Fellowship Award. All computations have been performed via the High Performance Computing (HPC) cluster provided by Queen Mary University of London⁸⁴.

Author contributions

G.D.B., I.I., A.P., and V.L. designed the study. A.P. performed a preliminary investigation, collected in an early draft. G.D.B. carried out the data collection and performed the numerical simulations. G.D.B., A.B., and G.D.M. carried out the analytical calculations. G.D.B., A.B., I.I., and V.L. wrote the manuscript. All authors contributed to analyze the data, discuss the results, define the proposed model, and revise the manuscript.

Competing interests

The authors declare no competing interests.

Additional information

Supplementary Information is attached to this manuscript.

Supplementary Information for “The dynamics of higher-order novelties”

S1 Higher-order Heaps’ exponents in the data sets

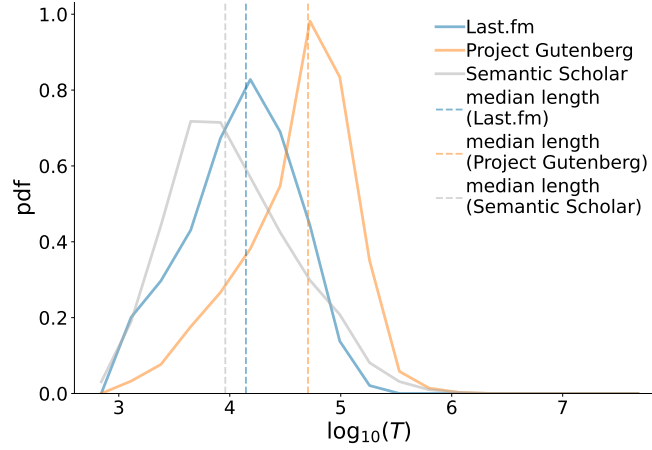


Figure S1. Length T distribution of the sequences in the data sets. Probability density function of the length T of all sequences in the three data sets (Last.fm in blue, Project Gutenberg in orange, Semantic Scholar in green). Moreover, the median lengths, respectively equal to 13 985, 50 726, and 9 114.5, are shown in the plot as vertical dashed lines, with the color corresponding to each data set.

data set (β_n)	min	1 st perc.	25 th perc.	median	75 th perc.	99 th perc.	max
Last.fm (β_1)	0.0007	0.0016	0.0052	0.0079	0.0129	0.0693	0.1988
Last.fm (β_2)	0.0000	0.0001	0.0026	0.0047	0.0091	0.0510	0.1497
Last.fm (β_3)	0.0000	0.0000	0.0019	0.0038	0.0073	0.0388	0.1366
Last.fm (β_4)	0.0000	0.0000	0.0015	0.0031	0.0064	0.0343	0.1294
Project Gutenberg (β_1)	0.0000	0.0010	0.0021	0.0029	0.0043	0.0169	0.0727
Project Gutenberg (β_2)	0.0003	0.0005	0.0010	0.0014	0.0020	0.0087	0.0522
Project Gutenberg (β_3)	0.0001	0.0002	0.0004	0.0006	0.0009	0.0064	0.0484
Project Gutenberg (β_4)	0.0000	0.0001	0.0001	0.0002	0.0005	0.0051	0.0444
Semantic Scholar (β_1)	0.0003	0.0008	0.0018	0.0025	0.0035	0.0115	0.1279
Semantic Scholar (β_2)	0.0002	0.0004	0.0010	0.0014	0.0021	0.0093	0.1677
Semantic Scholar (β_3)	0.0000	0.0002	0.0005	0.0008	0.0013	0.0078	0.1698
Semantic Scholar (β_4)	0.0000	0.0001	0.0003	0.0005	0.0009	0.0068	0.1620

Table S1. Statistics on the standard error of the fitted higher-order Heaps’ exponents in the empirical data. Various statistics on the standard error, or standard deviation of the estimator, of the fitted n^{th} -order Heaps’ exponents β_n of the sequences in the three data sets, with $n = 1, 2, 3$, and 4. Notice how the standard deviation of the distribution of the values of the exponents in the data sets (see Table. S2 for reference) is about two orders of magnitude higher than the median standard error and one order higher than its 99th percentile. Moreover, the p -values of the fits are all zero (not shown in the table).

data set (β_n)	mean	std	min	1 st perc.	25 th perc.	median	75 th perc.	99 th perc.	max
Last.fm (β_1)	0.7029	0.1797	0.1063	0.2010	0.5965	0.7395	0.8436	0.9761	0.9959
Last.fm (β_2)	0.9048	0.1014	0.3342	0.5725	0.8699	0.9388	0.9754	0.9999	0.9999
Last.fm (β_3)	0.9286	0.0862	0.3664	0.6123	0.9041	0.9583	0.9861	0.9999	1.0000
Last.fm (β_4)	0.9411	0.0759	0.3837	0.6643	0.9195	0.9679	0.9896	0.9999	1.0000
Project Gutenberg (β_1)	0.5699	0.0973	-0.0000	0.3678	0.5026	0.5594	0.6285	0.8302	0.9527
Project Gutenberg (β_2)	0.8527	0.0547	0.0304	0.7118	0.8191	0.8509	0.8883	0.9706	0.9919
Project Gutenberg (β_3)	0.9589	0.0300	0.0307	0.8648	0.9480	0.9627	0.9765	0.9968	0.9998
Project Gutenberg (β_4)	0.9882	0.0203	0.0304	0.9242	0.9870	0.9923	0.9958	0.9995	1.0000
Semantic Scholar (β_1)	0.6695	0.1019	0.2225	0.4673	0.5923	0.6590	0.7436	0.8889	0.9293
Semantic Scholar (β_2)	0.8895	0.0536	0.2587	0.7509	0.8550	0.8936	0.9303	0.9803	0.9942
Semantic Scholar (β_3)	0.9612	0.0305	0.2665	0.8686	0.9478	0.9680	0.9825	0.9972	0.9999
Semantic Scholar (β_4)	0.9847	0.0198	0.2790	0.9177	0.9807	0.9901	0.9954	0.9995	1.0000

Table S2. Statistics of the fitted higher-order Heaps' exponents in the data. Various statistics of the fitted n^{th} -order Heaps' exponents β_n of the sequences in the three data sets, with $n = 1, 2, 3$, and 4.

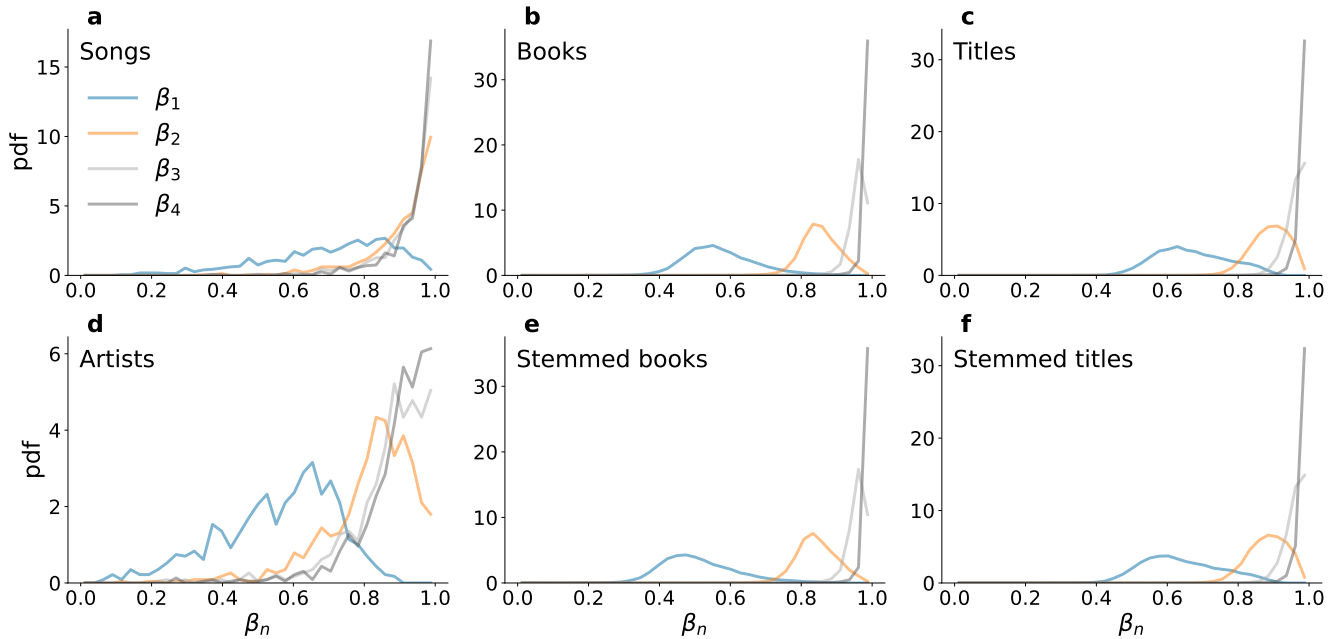
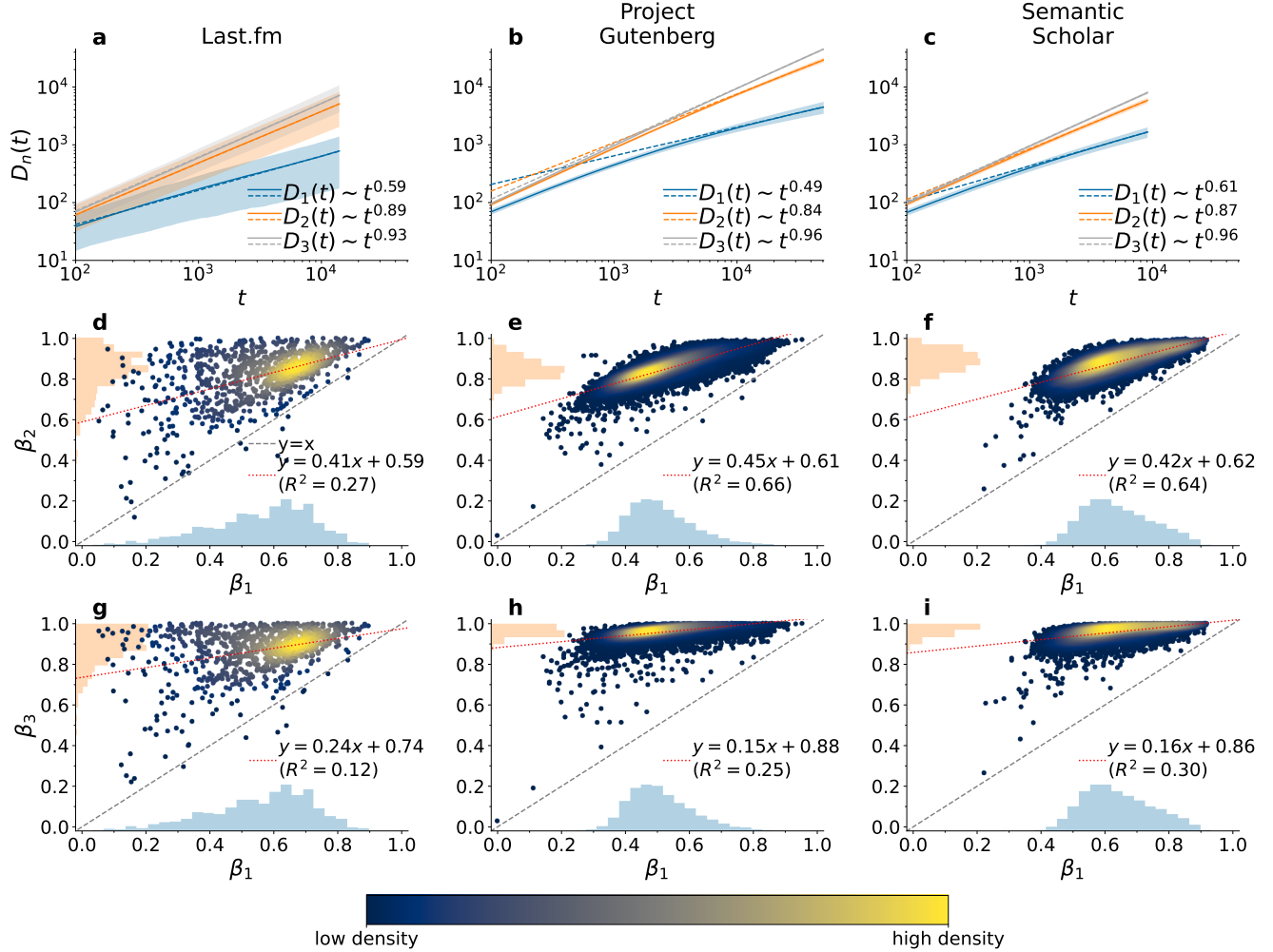


Figure S2. Heaps' exponent distribution of the sequences in the data sets. Probability density functions of the n^{th} -order Heaps' exponents β_n , with $n = 1, 2, 3, 4$, calculated from the empirical sequences (a-c) and respective sequences of labels (d-f). In particular, sequences contain songs (a) and artists (d) in Last.fm, words (b) and stemmed words (e) in Project Gutenberg books, words (c) and stemmed words (f) in Semantic Scholar journal titles.



S2 Heaps' exponents in simulations of the Urn Model with Semantic Triggering

The Urn Model with Triggering (UMT) features a triggering mechanism for the growth of the adjacent possible¹. In particular, whenever a new color is drawn for the first time, $v + 1$ new colors are triggered and added into the urn. Together with the reinforcement mechanism introduced in Polya's urn⁸⁰, the UMT manages to reproduce various features of innovation processes, including the Heaps' law. In particular, varying the parameters, the UMT produces different rates of discovery, which can be measured by the power-law exponent β_1 of the Heaps' law. According to analytical results on the asymptotic Heaps' exponent, we have that $\beta_1 \rightarrow v/\rho$. We check if this relation holds true at finite times in Fig. S4(a), where we show the scatter plots between v/ρ and the fitted value of β_1 for simulations of the UMT with $\rho = 20$ and $v = 1, \dots, 20$, run for $T = 10^5$ time steps. Each point refers to a different simulation, and we analyze 100 simulations for each set of parameters. We notice how the relationship holds true in most cases, although the fitted values are less than the theoretical ones, especially for high values of v/ρ . We repeat this check also for higher-order Heaps' exponents in Fig. S4(b-c), finding that also in this case there is not so much difference between the theoretical value v/ρ and the fitted β_2 and β_3 , if only that the points in the plot are slightly higher than the bisector.

We repeat the same analysis for the Urn Model with Semantic Triggering (UMST), which introduces semantic triggering between the colors in the urn. In particular, two colors are considered semantically related if they have been triggered by the same color (siblings) or if one has triggered the other (parent and child). Then, whenever a new color needs to be extracted, a ball of a certain color in the UMST has a different weight depending on the semantic relationship with the previous color. If the two colors are related, then the ball has weight 1, otherwise it gets weight $\eta \leq 1$. Analytical results on the Heaps' law from the SI in Ref.¹ show that the asymptotic Heaps' exponent is found between $\eta v/\rho$ and $\min(1, v/\rho)$. We test this in Fig. S4(d), where we show the scatter plots between $\eta v/\rho$ and the fitted value of β_1 for simulations of the UMST with $\rho = 4$ and $v = 1, \dots, 20$. We see that for low values of the $\eta v/\rho$ the value of β_1 corresponds to the theoretical lower bound. However, starting from about $\eta v/\rho = 0.2$ there are simulations in which the value of β_1 goes abruptly up to 1. Notice that for these values, we have that $v/\rho = 2$. Interestingly, up to $\eta v/\rho = 0.3$ and sometimes up to $\eta v/\rho = 0.4$, there are both simulations with Heaps' exponent $\beta_1 \approx \eta v/\rho$ and others with $\beta_1 \approx 1$, but almost none in between. After that, there remain only simulations

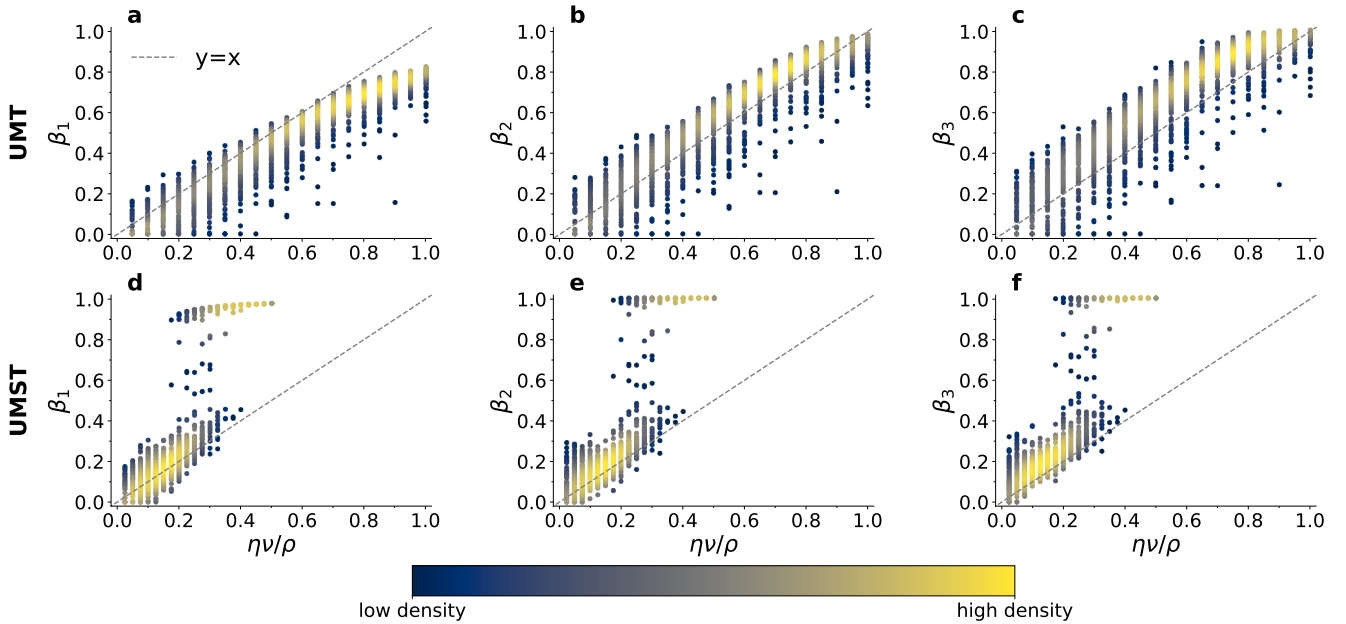


Figure S4. Higher-order Heaps' exponents and their correlations with the expected asymptotic value in urn model simulations. Scatter plots between the analytically expected lower bound $\eta v/\rho$ for the asymptotic 1st-order Heaps' exponent—the theoretical upper bound being $\min(1, v/\rho)$ —and the Heaps' exponents β_1 (a), β_2 (b), β_3 (c), β_4 (d). Each point refers to a different simulation of 10^5 time steps, colored according to the density of points (see color bar). Each panel reports the value of the correlation coefficient r . The first row refers to the Urn Model with Triggering (UMT), with no semantic correlations ($\eta = 1$) and $\rho = 20$. The second row refers to the Urn Model with Semantic Triggering (UMST), with $\rho = 4$ and $\eta = 0.1$. Here, we show the results of 100 simulations for each set of parameters.

η	ρ	ν	$\beta_1 \approx \eta\nu/\rho$	$\beta_1 \approx 1$
0.1	4	1	100	0
0.1	4	2	100	0
0.1	4	3	100	0
0.1	4	4	100	0
0.1	4	5	100	0
0.1	4	6	100	0
0.1	4	7	99	1
0.1	4	8	91	9
0.1	4	9	80	20
0.1	4	10	51	49
0.1	4	11	44	56
0.1	4	12	21	79
0.1	4	13	12	88
0.1	4	14	0	100
0.1	4	15	0	100
0.1	4	16	1	99
0.1	4	17	0	100
0.1	4	18	0	100
0.1	4	19	0	100
0.1	4	20	0	100

Table S3. Statistics on the number of simulations of urn models. Number of simulations of the UMST ($\eta = 0.1$, $\rho = 4$, $\nu = 1, \dots, 20$) that have an exponent approximately equal to the lower bound $\eta\nu/\rho$ or to the upper bound 1. For each set of parameters, 100 simulations have been launched.

with linear Heaps' law. We repeat the analysis for higher-order Heaps' exponents, finding the same behavior. In Table S3 we also report the number of simulations with either of the two behaviors. Notice how the number of simulations with $\beta_1 \approx 1$ increases with higher values of ν .

This analysis shows the inadequacy of the UMST to reproduce the whole spectrum of paces of discovery. In fact, we are not able to obtain Heaps' exponents in between the two theoretical limits. For example, we cannot obtain Heaps' exponents between roughly 0.4 and 0.9 when $\eta = 0.1$. Instead, simulations actually only produce exponents very close to these two bounds. Moreover, the higher the theoretical value $\eta\nu/\rho$, the higher the chance of having a Heaps' exponent close to 1. A possible explanation of why this could happen lies on the way semantic triggering happens. In the UMST, indeed, when a color is drawn for the first time, $\nu + 1$ balls of new colors are added to the urn, and they become semantically connected to the triggering color. Then, the probability to draw a ball of a color semantically close to the previous one is $1/\eta = 10$ times higher with respect to balls of other colors. This brings about two possible scenarios. On the one hand, if a small cluster of colors is highly reinforced in the beginning of the simulation, after one of them is drawn it is very likely that another of these colors is extracted in the next time step. On the other hand, if a new color is drawn, since it is highly probable to move to a semantic close color and almost all of them are new, if ν is high enough the next extracted color is also almost surely new. Then, once inside one of the two scenarios, it is very unlikely to break the loop, producing the two groups of Heaps' exponent we observe. This also explains why the likelihood of being in the linear case increases with ν , even though the two behaviors can coexist in the same set of parameters. Finally, this is also confirmed by simulations with higher number steps—we tested with 10^7 steps—, which show the same results, indicating that the behavior has already reached a stationary state.

S3 Analytic results for higher-order Heaps' exponents in UMT simulations

In this section we provide a complete analytical analysis of the higher-order Heaps' laws for the Urn Model with Triggering (UMT). Let us consider an urn with parameters ρ and ν and initially composed by $N_0 \geq 1$ balls of different colors.

S3.1 First-order Heaps' law

The evolution of the number $D_1(t)$ of different colors that have appeared in the first t positions of the sequence \mathcal{S} is ruled by the following master equation:

$$D_1(t+1) = D_1(t) + \mathbb{P}\left(\mathbb{N}^{(t+1)}\right) = D_1(t) + \frac{N_0 + \nu D_1(t)}{N_0 + \rho t + (\nu + 1)D_1(t)}, \quad (\text{S1})$$

where $\mathbb{N}^{(t+1)}$ is the event of drawing at time $(t+1)$ a ball of a color that has not been observed before. Its probability $\mathbb{P}\left(\mathbb{N}^{(t+1)}\right)$ can be expressed as the number of colors in the urn yet to be discovered, $N_0 + (\nu + 1)D_1(t) - D_1(t)$, divided by the total number of balls available at time t in the urn. In the long time limit, Eq. (S1) can be approximated by a differential equation, which leads to an analytical expression for $D_1(t)$ (see Refs. ^{1,52} for the analytical calculations):

$$\begin{cases} \frac{dD_1(t)}{dt} = \frac{N_0 + \nu D_1(t)}{N_0 + \rho t + (\nu + 1)D_1(t)} \\ D_1(0) = 0 \end{cases} \implies D_1(t) \underset{t \rightarrow \infty}{\approx} \begin{cases} bt^{\beta_1} & \text{if } \nu < \rho, \\ b \frac{t}{\log t} & \text{if } \nu = \rho, \\ bt & \text{if } \nu > \rho, \end{cases} \quad (\text{S2})$$

where $\beta_1 = \nu/\rho$ and b is a constant depending on ν and ρ . In other words, in the sublinear case $\nu < \rho$, the Heaps' law is analytically verified, with asymptotic exponent $\beta_1 = \nu/\rho$ ¹.

S3.2 Second-order Heaps' law

In order to write down an equation similar to Eq. (S2) for the the number $D_2(t)$ of different pairs that have appeared in the sequence \mathcal{S}_2 of length t , i.e.,

$$\begin{cases} \frac{dD_2(t)}{dt} = \mathbb{P}(\text{"The } t\text{-th pair is new"}), \\ D_2(0) = 0, \end{cases} \quad (\text{S3})$$

we need to calculate the probability to observe a new pair. However, differently from Eq. (S2), such a probability depends not only on the total number of balls and on the number of extracted colors, but also on the number of balls of each extracted color. Notice that the t -th pair (x_1, x_2) of \mathcal{S}_2 is composed by the color x_1 drawn at time t in \mathcal{S} and the color x_2 drawn in the next time step. Hence, there are three separate events in which the t -th pair (x_1, x_2) is a novelty in \mathcal{S}_2 : the event \mathbb{A} in which x_1 is a novelty, i.e. it appears for the first time in the sequence \mathcal{S} at time t ; the event \mathbb{B} in which x_1 is not a novelty but x_2 is a novelty; the event \mathbb{C} in which both colors x_1 and x_2 are not novel, but the combination (x_1, x_2) appears for the first time. Consequently, the probability that the t -th pair is new is equal to the sum of the probabilities of such events. Using Eq. (S2), for large values of t the probability of event \mathbb{A} can be written as

$$\mathbb{P}(\mathbb{A}) = \mathbb{P}\left(\mathbb{N}^{(t)}\right) = \frac{dD_1(t)}{dt} \underset{t \rightarrow \infty}{\approx} b\beta_1 t^{\beta_1-1}. \quad (\text{S4})$$

Similarly, denoting with $\overline{\mathbb{N}^{(t)}}$ the opposite event of $\mathbb{N}^{(t)}$, the probability of event \mathbb{B} reads

$$\mathbb{P}(\mathbb{B}) \approx \mathbb{P}\left(\overline{\mathbb{N}^{(t)}}\right) \mathbb{P}\left(\mathbb{N}^{(t+1)}\right) \approx \left(1 - \frac{dD_1(t)}{dt}\right) \frac{dD_1(t+1)}{dt} \approx b\beta_1 t^{\beta_1-1} = \mathbb{P}(\mathbb{A}), \quad (\text{S5})$$

where we have disregarded infinitesimals of lower order. Thirdly, we can compute the probability of the event \mathbb{C} by calculating the probability that each possible pair of old colors is a novelty in this time step. Since the number of old colors up to time t is $D_1(t)$, indicating with $\mathbb{C}_{i,j}^{(t)}$ the event in which i and j are two already extracted colors and their pair (i, j) is a novelty at time t in \mathcal{S}_2 , we can write:

$$\mathbb{P}(\mathbb{C}) \approx \mathbb{P}\left(\overline{\mathbb{N}^{(t)}}\right) \mathbb{P}\left(\overline{\mathbb{N}^{(t+1)}}\right) \mathbb{P}\left(\bigcup_{i,j=1}^{D_1(t)} \mathbb{C}_{i,j}^{(t)}\right) \approx \left(1 - b\beta_1 t^{\beta_1-1}\right)^2 \mathbb{P}\left(\bigcup_{i,j=1}^{bt^{\beta_1}} \mathbb{C}_{i,j}^{(t)}\right) \approx \sum_{i,j=1}^{bt^{\beta_1}} \mathbb{P}\left(\mathbb{C}_{i,j}^{(t)}\right). \quad (\text{S6})$$

The last equality in Eq. (S6) holds true because for any $(i_1, j_1) \neq (i_2, j_2)$ we have $\mathbb{C}_{i_1, j_1}^{(t)} \cap \mathbb{C}_{i_2, j_2}^{(t)} = \emptyset$, since only one pair can be extracted at each time step, and we have disregarded lower infinitesimals.

Let us now concentrate on computing the probability of $\mathbb{C}_{i, j}(t)$. Defining the event $\mathbb{E}_{ij}^{(\tau)}$ = “pair (i, j) appears (not necessarily for the first time) in the sequence at time τ ”, we can rewrite $\mathbb{C}_{i, j}^{(t)}$ as

$$\mathbb{C}_{i, j}^{(t)} = \overline{\mathbb{E}_{ij}^{(1)}} \cap \overline{\mathbb{E}_{ij}^{(2)}} \cap \dots \cap \overline{\mathbb{E}_{ij}^{(t-1)}} \cap \mathbb{E}_{ij}^{(t)}, \quad (\text{S7})$$

where we denote with $\overline{\mathbb{E}_{ij}^{(\tau)}}$ the opposite event of $\mathbb{E}_{ij}^{(\tau)}$. We can hence compute its probability as

$$\begin{aligned} \mathbb{P}(\mathbb{C}_{i, j}^{(t)}) &= \mathbb{P}(\overline{\mathbb{E}_{ij}^{(1)}} \cap \overline{\mathbb{E}_{ij}^{(2)}} \cap \dots \cap \overline{\mathbb{E}_{ij}^{(t-1)}} \cap \mathbb{E}_{ij}^{(t)}) \\ &= \mathbb{P}(\overline{\mathbb{E}_{ij}^{(1)}}) \mathbb{P}(\overline{\mathbb{E}_{ij}^{(2)}} | \overline{\mathbb{E}_{ij}^{(1)}}) \dots \mathbb{P}(\overline{\mathbb{E}_{ij}^{(t-1)}} | \overline{\mathbb{E}_{ij}^{(1)}} \cap \dots \cap \overline{\mathbb{E}_{ij}^{(t-2)}}) \mathbb{P}(\mathbb{E}_{ij}^{(t)} | \overline{\mathbb{E}_{ij}^{(1)}} \cap \dots \cap \overline{\mathbb{E}_{ij}^{(t-1)}}). \end{aligned} \quad (\text{S8})$$

First, we notice that we can simplify the expressions in Eq. (S8), since

$$\mathbb{P}(\mathbb{E}_{ij}^{(\tau)} | \overline{\mathbb{E}_{ij}^{(1)}} \cap \dots \cap \overline{\mathbb{E}_{ij}^{(\tau-1)}}) = \mathbb{P}(\mathbb{E}_{ij}^{(\tau)} | \overline{\mathbb{E}_{ij}^{(\tau-1)}}). \quad (\text{S9})$$

This equality in Eq. (S9) holds true because, the probability of extracting the pair (i, j) at time τ can only be influenced by what has happened at time $(\tau - 1)$, disregarding all previous times.

Without loss of generality, let us index the colors in the urn in the same order they first appeared in the sequence, i.e., let us suppose that the i -th color has appeared at time t_i , with $t_{i+1} > t_i$, for $i = 1, 2, \dots, D_1(t)$. Let us also suppose that the rate at which a new color appears is given exactly by the approximated solution given by Eq. (S2). Then, it would be

$$i = D(t_i) \approx b t_i^{\beta_1} \implies t_i \approx \left(\frac{i}{b}\right)^{\frac{1}{\beta_1}}. \quad (\text{S10})$$

With Eq. (S10) we are assuming that the behaviour of $D_1(t)$ at finite times can be approximated with the asymptotic one, and that colors appear deterministically at these expected moments. Even though strong, this assumption makes sense if we consider that, as it has been observed before, there is a good correspondence between this analytical solution and simulations at finite times. Moreover, we will confirm *a posteriori* the suitability of this assumption since, as we will see, there is correspondence between the analytical solution of $D_2(t)$ we obtain here and the results of model simulations.

Let us now define $n_i(t)$ as the number of times the color i has appeared before time t , supposing it has first appeared at time $t_i \leq t$. If $\mathbb{E}_i^{(t)}$ = “ i appears at time t ” (not necessarily for the first time), then we have that $\frac{dn_i}{dt} = \mathbb{P}(\mathbb{E}_i^{(t)})$. Thus, we can write:

$$\begin{cases} \frac{dn_i(t)}{dt} = \frac{\rho n_i(t) + 1}{N_0 + aD(t) + \rho t} \underset{t \rightarrow \infty}{\approx} \frac{n_i}{t}, \\ n_i(t_i) = 1, \end{cases} \implies \begin{cases} n_i(t) \underset{t \rightarrow \infty}{\approx} \frac{t}{t_i} & \text{if } t \geq t_i, \\ n_i(t) = 0 & \text{if } t < t_i, \end{cases} \implies \begin{cases} \frac{dn_i(t)}{dt} \underset{t \rightarrow \infty}{\approx} \frac{1}{t_i} = \left(\frac{b}{i}\right)^{\frac{1}{\beta_1}} & \text{if } t \geq t_i, \\ \frac{dn_i(t)}{dt} = 0 & \text{if } t < t_i. \end{cases} \quad (\text{S11})$$

Let us observe that under these assumptions dn_i/dt is actually constant in time, depending just on t_i .

Then, supposing that the number of balls $n_i(\tau)$, $n_j(\tau)$ of the two colors in the urn follows exactly Eq. (S3), we can calculate the probability of $\mathbb{E}_{ij}^{(\tau)}$ as

$$\mathbb{P}(\mathbb{E}_{ij}^{(\tau)}) = \mathbb{P}(\mathbb{E}_i^{(\tau)}) \mathbb{P}(\mathbb{E}_j^{(\tau+1)}) = \frac{dn_i(\tau)}{d\tau} \frac{dn_j(\tau+1)}{d\tau} \underset{t \rightarrow \infty}{\approx} \begin{cases} \frac{1}{t_i t_j} & \text{if } \tau \geq \max(t_i, t_j - 1), \\ 0 & \text{if } \tau < \max(t_i, t_j - 1). \end{cases} \quad (\text{S12})$$

Furthermore, if $\tau \geq \max(t_i, t_j - 1)$, we can write

$$\begin{aligned}
\mathbb{P}\left(\mathbb{E}_{ij}^{(\tau)} \cap \overline{\mathbb{E}_{ij}^{(\tau-1)}}\right) &= \mathbb{P}\left(\left[\left(\mathbb{E}_{ij}^{(\tau+1)} \cap \overline{\mathbb{E}_{ij}^{(\tau)}}\right) \cap \mathbb{E}_j^{(\tau)}\right] \cup \left[\left(\mathbb{E}_{ij}^{(\tau+1)} \cap \overline{\mathbb{E}_{ij}^{(\tau)}}\right) \cap \overline{\mathbb{E}_j^{(\tau)}}\right]\right) \\
&= \mathbb{P}\left(\left[\mathbb{E}_i^{(\tau)} \cap \mathbb{E}_j^{(\tau+1)} \cap \overline{\mathbb{E}_i^{(\tau-1)}} \cap \mathbb{E}_j^{(\tau)}\right] \cup \left[\mathbb{E}_i^{(\tau)} \cap \mathbb{E}_j^{(\tau+1)} \cap \overline{\mathbb{E}_j^{(\tau)}}\right]\right) \\
&= \mathbb{P}\left(\mathbb{E}_i^{(\tau)} \cap \mathbb{E}_j^{(\tau)}\right) \mathbb{P}\left(\mathbb{E}_j^{(\tau+1)}\right) \mathbb{P}\left(\overline{\mathbb{E}_i^{(\tau-1)}}\right) + \mathbb{P}\left(\mathbb{E}_i^{(\tau)} \cap \overline{\mathbb{E}_j^{(\tau)}}\right) \mathbb{P}\left(\mathbb{E}_j^{(\tau+1)}\right) \\
&= \delta(i, j) \frac{1}{t_i} \frac{1}{t_j} \left(1 - \frac{1}{t_i}\right) + (1 - \delta(i, j)) \frac{1}{t_i} \frac{1}{t_j}.
\end{aligned} \tag{S13}$$

Therefore, we get

$$\begin{aligned}
\mathbb{P}\left(\mathbb{E}_{ij}^{(\tau)} \mid \overline{\mathbb{E}_{ij}^{(\tau-1)}}\right) &= \frac{\mathbb{P}\left(\mathbb{E}_{ij}^{(\tau)} \cap \overline{\mathbb{E}_{ij}^{(\tau-1)}}\right)}{\mathbb{P}\left(\overline{\mathbb{E}_{ij}^{(\tau-1)}}\right)} = \frac{\delta(i, j) \frac{1}{t_i t_j} \left(1 - \frac{1}{t_i}\right) + \frac{1 - \delta(i, j)}{t_i t_j}}{1 - \frac{1}{t_i t_j}} \\
&= \frac{\delta(i, j) \left(1 - \frac{1}{t_i}\right) + (1 - \delta(i, j))}{t_i t_j - 1} = \delta(i, j) \frac{\left(1 - \frac{1}{t_i}\right)}{t_i t_j - 1} + (1 - \delta(i, j)) \frac{1}{t_i t_j - 1} \\
&= \delta(i, j) \frac{1}{t_i^2 + t_i} + (1 - \delta(i, j)) \frac{1}{t_i t_j - 1}.
\end{aligned} \tag{S14}$$

In the following of this discussion, we make the following approximation:

$$\delta(i, j) \frac{1}{t_i^2 + t_i} + (1 - \delta(i, j)) \frac{1}{t_i t_j - 1} \approx \frac{1}{t_i t_j}. \tag{S15}$$

Because of Eq. (S12), the approximation in Eq. (S15) implies in Eq. (S14) that

$$\mathbb{P}\left(\mathbb{E}_{ij}^{(\tau)} \mid \overline{\mathbb{E}_{ij}^{(\tau-1)}}\right) \approx \begin{cases} \frac{1}{t_i t_j} & \text{if } \tau \geq \max(t_i, t_j - 1) \\ 0 & \text{if } \tau < \max(t_i, t_j - 1) \end{cases} \implies \mathbb{P}\left(\mathbb{E}_{ij}^{(\tau)} \mid \overline{\mathbb{E}_{ij}^{(\tau-1)}}\right) \approx \mathbb{P}\left(\mathbb{E}_{ij}^{(\tau)}\right), \tag{S16}$$

which is equivalent to assume that $\mathbb{E}_{ij}^{(\tau)}$ and $\overline{\mathbb{E}_{ij}^{(\tau-1)}}$ are statistically independent, i.e. that the extraction of a certain pair (i, j) at time τ is independent of its extraction at the previous time $(\tau - 1)$. Therefore, using Eq. (S8), Eq. (S9), Eq. (S12) and Eq. (S16), the probability of the event $\mathbb{C}_{ij}^{(t)}$ that the pair (i, j) is extracted at time t for the first time can be approximated to

$$\begin{aligned}
\mathbb{P}\left(\mathbb{C}_{ij}^{(t)}\right) &= \mathbb{P}\left(\overline{\mathbb{E}_{ij}^{(1)}}\right) \mathbb{P}\left(\overline{\mathbb{E}_{ij}^{(2)}}\right) \cdots \mathbb{P}\left(\overline{\mathbb{E}_{ij}^{(t-1)}}\right) \mathbb{P}\left(\mathbb{E}_{ij}^{(t)}\right) = \prod_{\tau=1}^{t-1} \mathbb{P}\left(\overline{\mathbb{E}_{ij}^{(\tau)}}\right) \mathbb{P}\left(\mathbb{E}_{ij}^{(t)}\right) \\
&= \prod_{\tau=\max(t_i, t_j-1)}^{t-1} \left(1 - \mathbb{P}\left(\mathbb{E}_{ij}^{(\tau)}\right)\right) \mathbb{P}\left(\mathbb{E}_{ij}^{(t)}\right) = \left(1 - \frac{1}{t_i t_j}\right)^{t-\max(t_i, t_j-1)} \frac{1}{t_i t_j},
\end{aligned} \tag{S17}$$

which can be used in Eq. (S6) to obtain an approximated expression for the probability of event \mathbb{C} , i.e.,

$$\mathbb{P}(\mathbb{C}) \approx \sum_{i,j=1}^{b t \beta_1} \mathbb{P}\left(\mathbb{C}_{ij}^{(t)}\right) \approx \sum_{i,j=1}^{b t \beta_1} \left(1 - \frac{1}{t_i t_j}\right)^{t-\max(t_i, t_j-1)} \frac{1}{t_i t_j}. \tag{S18}$$

Summing up, by inserting Eq. (S4), Eq. (S5), and Eq. (S18) into Eq. (S3), we get the following differential equation for the number of new pairs in time in the UMT:

$$\frac{dD_2}{dt} \underset{t \rightarrow \infty}{\approx} \underbrace{2b\beta_1 t^{\beta_1-1} + \sum_{i,j=1}^{b t \beta_1} \left(1 - \frac{1}{t_i t_j}\right)^{t-\max(t_i, t_j-1)} \frac{1}{t_i t_j}}_{\mathcal{C}(t)}. \tag{S19}$$

In order to have an estimate of $\mathcal{C}(t)$, let us approximate the sum with the related integral:

$$\mathcal{C}(t) \underset{t \rightarrow \infty}{\approx} \int_1^{bt^{\beta_1}} \int_1^{bt^{\beta_1}} \left(1 - \frac{1}{t_x t_y}\right)^{t - \max(t_x, t_y - 1)} \frac{1}{t_x t_y} dx dy. \quad (\text{S20})$$

This way, using the change of variables $u = t_x = \left(\frac{x}{b}\right)^{\frac{1}{\beta_1}}$, $v = t_y = \left(\frac{y}{b}\right)^{\frac{1}{\beta_1}}$, we get

$$\mathcal{C}(t) \underset{t \rightarrow \infty}{\approx} (b\beta_1)^2 \int_{\frac{1}{\rho-v}}^t \int_{\frac{1}{\rho-v}}^t \left(1 - \frac{1}{uv}\right)^{t - \max(u, v-1)} \frac{du dv}{(uv)^{2-\beta_1}}, \quad (\text{S21})$$

where we have substituted the initial value $\left(\frac{1}{b}\right)^{\frac{1}{\beta_1}} = \frac{1}{\rho-v}$, since $b = (\rho-v)^{\beta_1}$ when $v < \rho$, that is in this case¹. Moreover, considering that u and v represent time variables, with $\tau \in (1, t)$, since between $t = 0$ and $t = 1$ there are no colors extracted yet, we can change the lower integral border to 1, i.e.,

$$\mathcal{C}(t) \underset{t \rightarrow \infty}{\approx} (b\beta_1)^2 \int_1^t \int_1^t \left(1 - \frac{1}{uv}\right)^{t - \max(u, v)} \frac{du dv}{(uv)^{2-\beta_1}}, \quad (\text{S22})$$

where we have also simplified the exponent in the integrand, so that we can more easily calculate it as

$$\mathcal{C}(t) \underset{t \rightarrow \infty}{\approx} 2(b\beta_1)^2 \int_1^t \int_1^u \left(1 - \frac{1}{uv}\right)^{t-u} \frac{du dv}{(uv)^{2-\beta_1}}. \quad (\text{S23})$$

We numerically solve the integral in Eq. (S23) on specified points t_i using the command `NIntegrate` of *Mathematica*⁸⁵. The points t_i have been chosen on a fine logarithmically spaced grid of $N = 1601$ points $1 = t_0 < t_1 < \dots < t_N = 10^{16}$. By plugging the numerical approximation $\mathcal{C}(t_i)$ into Eq. (S19), we also obtain a numerical approximation of dD_2/dt in these points. We also obtain an analytical approximation of dD_2/dt by fitting a function of the type $at^{b+c/(d+\log_2(t))}$ using `curve_fit` (in *Python*'s package `scipy`), where the minimization of the error has been done in logarithm scale. Finally, integrating Eq. (S19) over t , we obtain a solution for $D_2(t)$. Again, we are not able to solve this integral analytically, so we solve it numerically using the analytical fit of dD_2/dt . In particular, we integrate using *Python*'s command `odeint` in the `scipy` package. We find that the numerical integration for $D_2(t)$ can also be fitted by a function of the type $at^{\beta_1+c/(d+\log_2(t))}$.

To sum up, we have derived a solution of Eq. (S19) of the type

$$D_2(t) \approx at^{\beta_2}, \quad \text{with } \beta_2 = \beta_1 + \frac{c}{d + \log(t)}, \quad (\text{S24})$$

where a , c , and d depend on the parameters ρ and v . Fig. S5 shows that the analytical expression of β_2 we have found is in good agreement with the numerical simulations. From left to right, we consider parameters $\rho = 4$ and $v = 1, 2, 3$, and we run simulations until $T = 10^7$. In each plot, continuous lines represent the 2nd-order Heaps' exponents of the power-law fits as a function of time t . The continuous blue line is obtained by fitting the best parameters a , c and d that minimize the error between the points $D_2(t)$ of the simulations with a function of the type $at^{\beta_1 + \frac{c}{d + \log(t)}}$. The continuous orange line instead represents the result of our analytical approach in Eq. (S24). The expected value of $\beta_1 = v/\rho$ is represented as a horizontal dashed gray line. Our results further confirm that 2nd-order Heaps' exponents differ from the 1st-order ones at finite times. However, they also highlight that in the UMT the difference between β_2 and β_1 slowly decays in time.

S3.3 Higher-order Heaps' law

Finally, we point out that an analytical solution for higher-order Heaps' exponents can also be obtained by induction, with assumptions similar to those used for the 2nd-order one. For example, for the 3rd-order, we can repeat the same process as in Sec. S3.2 to compute the probabilities of obtaining a new triplet. In particular, supposing that

$$\frac{dD_1(t)}{dt} \approx a_1 t^{\beta_1-1}, \quad \frac{dD_2(t)}{dt} \approx a_2 t^{\beta_1-1 + \frac{c_2}{d_2 + \log_2(t)}}, \quad (\text{S25})$$

we can obtain a new triplet in the three following distinct cases.

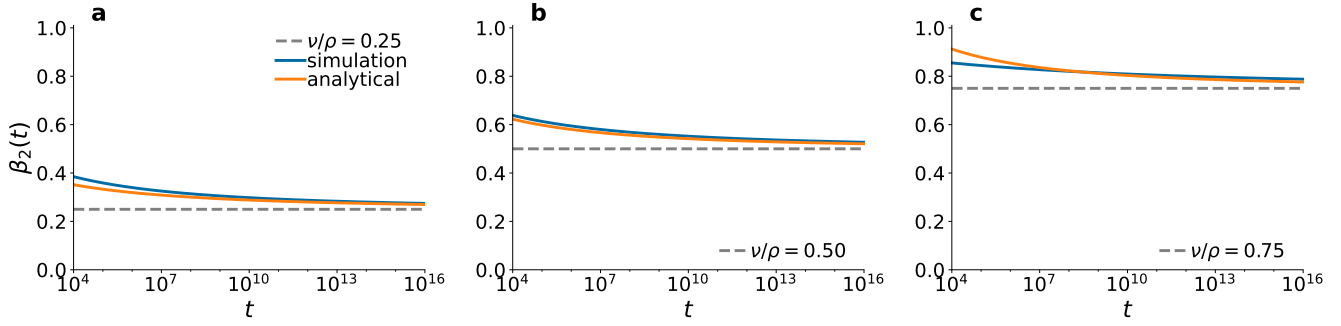


Figure S5. 2nd-order Heaps' exponent in the urn model with triggering. Temporal evolution of the 2nd-order Heaps' exponents $\beta_2(t)$ of the urn model with triggering according to the simulations (continuous blue line) and the numerical integration of Eq. (S19) (continuous orange line). Parameters are set to $\rho = 4$ and $\eta = 1$, while v varies across panels: $v = 1$ (a), 2 (b), and 3 (c). Continuous lines are obtained by fitting $D_2(t)$ with a function $at^{\beta_1+c/(d+\log_2(t))}$, as in Eq. (S24). The expected 1st-order Heaps' exponent in each panel, respectively equal to $\beta_1 = v/\rho = 0.25, 0.5, 0.75$, is displayed as a dashed gray horizontal line.

(A): when at time $(t-1)$ a new pair is drawn, which happens with probability

$$\mathbb{P}(\text{A}) = \frac{dD_2(t-1)}{dt} \approx a_2 t^{\beta_1-1+\frac{c_2}{d_2+\log_2(t)}}. \quad (\text{S26})$$

(B): when at time $(t-1)$ an old pair is drawn, and at time t a new color is drawn, which happens with probability

$$\mathbb{P}(\text{B}) = \left(1 - \frac{dD_2(t-1)}{dt}\right) \frac{dD_1(t)}{dt} \approx \left(1 - a_2 t^{\beta_1-1+c_2/(d_2+\log_2(t))}\right) a_1 t^{\beta_1-1} \approx a_1 t^{\beta_1-1}. \quad (\text{S27})$$

(C): when at both times $(t-1)$ and t an old pair and an old color are extracted, but the corresponding triplet has never appeared in the sequence before. Following the same steps of the 2nd-order case, we get the probability

$$\begin{aligned} \mathbb{P}(\text{C}) &\approx \sum_{i,j,k=1}^{bt^{\beta_1}} \left(1 - \frac{1}{t_i t_j t_k}\right)^{t-\max(t_i, t_j, t_k)} \frac{1}{t_i t_j t_k} \approx \\ &\approx (a_1)^3 \int_1^t \int_1^t \int_1^t \left(1 - \frac{1}{uvw}\right)^{t-\max(u, v-1, w-2)} \frac{du dv dw}{(uvw)^{2-\beta_1}} \approx \\ &\approx 3! (a_1)^3 \int_1^t \int_1^u \int_1^v \left(1 - \frac{1}{uvw}\right)^{t-u} \frac{du dv dw}{(uvw)^{2-\beta_1}}, \end{aligned} \quad (\text{S28})$$

where $3! = 3 \cdot 2 \cdot 1$.

Then, summing up Eq. (S26), Eq. (S27) and Eq. (S28), the probability to have a new triplet can be approximated as

$$\frac{dD_3(t)}{dt} \approx a_2 t^{\beta_1-1+\frac{c_2}{d_2+\log_2(t)}} + a_1 t^{\beta_1-1} + 3! (a_1)^3 \int_1^t \int_1^u \int_1^v \left(1 - \frac{1}{uvw}\right)^{t-u} \frac{du dv dw}{(uvw)^{2-\beta_1}}. \quad (\text{S29})$$

In general, for the n^{th} -order Heaps' law, let us suppose by induction that all lower orders are known, i.e., for all orders $k = 1, \dots, n-1$, with $n \geq 2$, we have

$$\frac{dD_k(t)}{dt} \approx a_k t^{\beta_1-1+\frac{c_k}{d_k+\log_2(t)}}, \quad D_k(t) = \tilde{a}_k t^{\beta_1+\frac{c_k}{d_k+\log_2(t)}}, \quad (\text{S30})$$

with $a, c, d > 0$. Then, following the same procedure used for the 3rd-order Heaps' law, the probability of extracting a new n -tuple is given by:

$$\frac{dD_n(t)}{dt} \approx \frac{dD_{n-1}(t)}{dt} + \frac{dD_1(t)}{dt} + n! (a_1)^n \underbrace{\int_1^t \int_1^{u_1} \cdots \int_1^{u_{n-1}}}_{n \text{ integrals}} \left(1 - \frac{1}{u_1 \cdots u_n}\right)^{t-u_1} \frac{du_1 \cdots du_n}{(u_1 \cdots u_n)^{2-\beta_1}}, \quad (\text{S31})$$

which approximately gives

$$\frac{dD_n(t)}{dt} \approx a_n t^{\beta_1 - 1 + \frac{c_n}{d_n + \log_2(t)}}, \quad D_n(t) = \tilde{a}_n t^{\beta_1 + \frac{c_n}{d_n + \log_2(t)}}. \quad (\text{S32})$$

S4 Analytical details of ERRWT model

In this section we provide an analytical insight of the model proposed in this manuscript, the Edge-Reinforced Random Walk with Triggering, or ERRWT. In particular, we refer to the definition of the ERRWT model given in *Materials and Methods* in the main manuscript, and try to build differential equations for the evolution of $D_1(t)$ and $D_2(t)$. From now on, we omit the explicit time dependence of the variables, e.g., $D_1 \equiv D_1(t)$, so that the mathematical expressions are easier to read.

In the following analysis we make an important simplification, that is, we do not consider an undirected update as defined the main text. Undirected update means that at any time a new link (i, j) is reinforced or triggered, the link (j, i) is updated as well; here we consider the directed version of the model (only the visited link (i, j) is updated).

We start from considering variables referring to single nodes: $D_{1i}^{in}, D_{1i}^{out}, D_{2i}^{in}, D_{2i}^{out}$ represent respectively the number of times a new node is discovered *arriving (in)* in node i , and *leaving (out)* from node i , and the same for the number of times a new link is discovered arriving or leaving from node i . Notice that D_{1i}^{in} becomes 1 as soon as node i is visited for the first time.

These micro variables can be aggregated to obtain the macro variables D_1 and D_2 , considering either *in* or *out* variables and summing over all the nodes:

$$D_1 = \sum_i D_{1i}^{in} = \sum_i D_{1i}^{out} \quad D_2 = \sum_i D_{2i}^{in} = \sum_i D_{2i}^{out} \quad (S33)$$

Let us now build differential equations for the evolution of the micro variables, which will be aggregated to obtain self-consistent equations for D_1 and D_2 . Let us consider the probability of exploring a new node starting from node i , i.e., the probability that the variable D_{1i}^{out} increases by 1. On the one hand, the total weight of the links outgoing from node i is equal to

$$M_{0i} + \rho n_i + (v_1 + 1)D_{1i}^{in} + (v_2 + 1)D_{2i}^{in}, \quad (S34)$$

where M_{0i} is the initial number of links connected with node i at time $t = 0$, and $n_i \equiv n_i(t)$ is the number of times node i has been visited up to time t . The other two terms refer to the new links triggered when arriving in node i . Indeed, when i is visited for the first time, $(v_1 + 1)$ links outgoing from i to new nodes are triggered. Moreover, whenever a link ending in i is traversed for the first time, $(v_2 + 1)$ new links from i to other explored nodes are triggered. On the other hand the total weight of links connecting i and never explored nodes is equal to

$$M_{0i} + (v_1 + 1)D_{1i}^{in} - D_{1i}^{out}, \quad (S35)$$

i.e., the initial number of nodes connected to i yet to be discovered, plus the number of nodes triggered when discovering node i , minus the number of nodes already discovered starting from i . These considerations make possible to write that

$$\frac{dD_{1i}^{out}}{dt} = p(i, t) \frac{M_{0i} + (v_1 + 1)D_{1i}^{in} - D_{1i}^{out}}{M_{0i} + \rho n_i + (v_1 + 1)D_{1i}^{in} + (v_2 + 1)D_{2i}^{in}}, \quad (S36)$$

where $p(i, t)$ is the probability of being on node i at time t , which is a needed condition for D_{1i}^{out} to evolve. Using the same argument, we can also write an equation for the evolution of D_{2i}^{out} :

$$\frac{dD_{2i}^{out}}{dt} = p(i, t) \frac{M_{0i} + (v_1 + 1)D_{1i}^{in} + (v_2 + 1)D_{2i}^{in} - D_{2i}^{out}}{M_{0i} + \rho n_i + (v_1 + 1)D_{1i}^{in} + (v_2 + 1)D_{2i}^{in}} \quad (S37)$$

Notice that Eq. (S36) and Eq. (S37) cannot be obtained so easily in the undirected case. In fact, here we have implicitly assumed that any link in the adjacent possible that has never been visited before has weight 1. However, if the update is undirected, we may reinforce some link (j, i) never traversed before only because the walker might have visited the edge (i, j) , making impossible to know the actual weight of never traversed links.

At this point we make another assumption in order to make the equations solvable. In particular, we assume a precise expression for the variable n_i . In fact, as we have seen in Sec. S3, in the UMT, at least in the sublinear regime, we have $n_i(t) \sim t/t_i$, where t_i is the first time item (node) i has been visited¹. Exploiting the analogy between the UMT and the ERRWT model we assume that $n_i(t)$ has the same behaviour. We also checked numerically the validity of this assumption. We have indeed measured the evolution of $n_i(t)$ in simulations of the ERRWT model, showing that the assumption is reasonable for very different values of the parameters v_1 and v_2 , as shown in Fig. S6. Further notice that $p(i, t) = dn_i(t - 1)/dt \approx 1/t_i$, since the probability of being on i at time t is equal to the probability to move to node i in the previous time step. With all these elements we can rewrite Eq. (S36) and Eq. (S37) as

$$\frac{dD_{1i}^{out}}{dt} \approx \frac{1}{t_i} \frac{M_{0i} + (v_1 + 1)D_{1i}^{in} - D_{1i}^{out}}{M_{0i} + \rho \frac{t}{t_i} + (v_1 + 1)D_{1i}^{in} + (v_2 + 1)D_{2i}^{in}} \quad (S38)$$

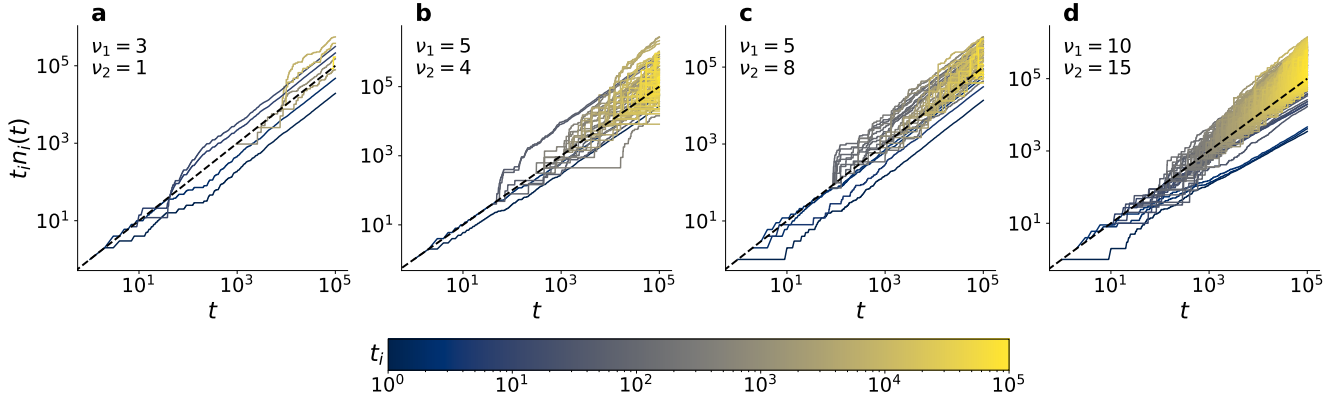


Figure S6. Temporal evolution of the quantities $n_i(t)$. In these figures we show the temporal evolution of $n_i(t)$, i.e. the number of times node i has been explored at time t , for many choices of the node i . In order to check the assumption $n_i(t) \sim t/t_i$, where t_i is the time when node i is discovered for the first time, we actually plotted $t_i n_i(t)$ vs t . We expect this quantity to go like t , which is represented by the dotted black line. As we can see from the four panels, the assumption is valid for a wide range of the parameters v_1 and v_2 .

and

$$\frac{dD_{2i}^{out}}{dt} \approx \frac{1}{t_i} \frac{M_{0i} + (v_1 + 1)D_{1i}^{in} + (v_2 + 1)D_{2i}^{in} - D_{2i}^{out}}{M_{0i} + \rho \frac{t}{t_i} + (v_1 + 1)D_{1i}^{in} + (v_2 + 1)D_{2i}^{in}}. \quad (S39)$$

The last step before aggregating the equations is to further simplify the denominator. First notice that D_{1i}^{in} is a variable which can only take values 0 or 1, since an arriving node can result to be new only one time (this is not true for D_{1i}^{out} , which can be larger than 1). So we can neglect it with respect to the term with D_{2i}^{in} , because also this can be larger than 1 and can go to infinity with time with a pace dependent on the parameters as we will see later. Finally, we assume $D_{2i}^{in} \approx D_2/t_i$; this is a reasonable assumption given the fact that $n_i(t) \approx t/t_i$. Indeed, if a node i is visited with a frequency depending on the inverse of t_i , it is reasonable to assume that also the number of new links traversed arriving in node i occurs with the same frequency as well.

We can finally aggregate the equations summing over all nodes i obtaining a self consistent equation for the evolution of D_1 :

$$\begin{aligned} \frac{dD_1}{dt} &= \sum_{i=1}^{D_1} \frac{dD_{1i}^{out}}{dt} \approx \sum_i \frac{1}{t_i} \frac{M_{0i} + (v_1 + 1)D_{1i}^{in} - D_{1i}^{out}}{\rho \frac{t}{t_i} + (v_2 + 1) \frac{D_2}{t_i}} \approx \sum_i \frac{M_{0i} + (v_1 + 1)D_{1i}^{in} - D_{1i}^{out}}{\rho t + (v_2 + 1)D_2} \\ &= \frac{M_0 + (v_1 + 1)D_1 - D_1}{\rho t + (v_2 + 1)D_2} \approx \frac{v_1 D_1}{\rho t + (v_2 + 1)D_2}, \end{aligned} \quad (S40)$$

where in the last approximation we have disregarded M_0 in the numerator since $D_1(t) \rightarrow \infty$ is the leading term in the numerator. Similarly for the 2nd-order Heaps' law we can write

$$\begin{aligned} \frac{dD_2}{dt} &= \sum_{i=1}^{D_1} \frac{dD_{2i}^{out}}{dt} \approx \sum_{i=1}^{D_1} \frac{1}{t_i} \frac{M_{0i} + (v_1 + 1)D_{1i}^{in} + (v_2 + 1)D_{2i}^{in} - D_{2i}^{out}}{\rho \frac{t}{t_i} + (v_2 + 1) \frac{D_2}{t_i}} \\ &= \frac{M_0 + (v_1 + 1)D_1 + (v_2 + 1)D_2 - D_2}{\rho t + (v_2 + 1)D_2} \approx \frac{(v_1 + 1)D_1 + v_2 D_2}{\rho t + (v_2 + 1)D_2}. \end{aligned} \quad (S41)$$

Notice that the initial structure of the network only enters in the equations through the constant $M_0 \equiv \sum_i M_{0i}$, and as we already said this term can be safely neglected with respect to the other variables. This means that the asymptotic behaviour of D_1 and D_2 , and so the exponents β_1 and β_2 , should not depend on the initial structure of the network. We checked this fact running simulations with different initial conditions and measuring the exponents β_1 and β_2 , checking that we obtain similar result in all cases. The results of this analysis is shown in Fig. S7. In particular, we consider regular trees with different number of levels, but same branching size. The idea is that we start from a node and trigger nodes, adding new levels of the tree.

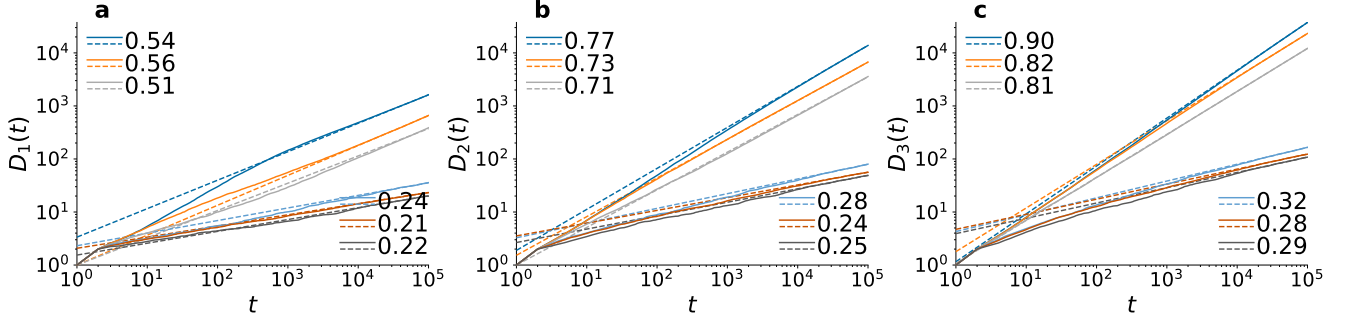


Figure S7. Heaps' exponents for different choices of the initial conditions. The three panels show the behaviour of $D_1(t)$, $D_2(t)$ and $D_3(t)$ versus t for three different initial conditions (i.e., initial structure of the network). In particular, we consider a regular tree with branching parameter $v_1 + 1$ and number of levels equal to 1 (gray lines), 2 (orange lines), 3 (blue lines). All nodes apart from the leaves are considered known (or discovered, or triggered) by the ERRWT at the beginning of the simulation. In each panel, the lines with higher Heaps' law (see top left legend), refer to simulations with $\rho = 10$, $v_1 = 8$, and $v_2 = 8$, while the other lines (see bottom right legend) with $\rho = 10$, $v_1 = 3$, and $v_2 = 1$. In the legend, the related extracted power-law exponent is reported. As we can see, the exponents measured in the three cases are similar across order, thus showing that the initial structure of the network is not relevant for the asymptotic behaviour of the ERRWT.

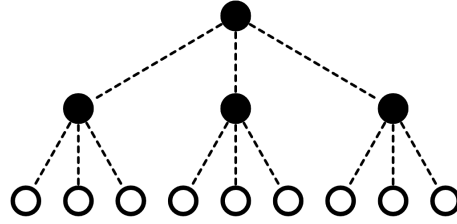


Figure S8. Representation of the initial network structure used in simulations of the ERRWT model in the main.

Although any initial network structure can be used for the ERRWT model, in the simulations shown in the main manuscript we consider a regular tree with branching parameter $v_1 + 1$ (equal to 3 in the figure) and 2 levels. This structure resembles the way new nodes are triggered during the exploration, so that the root and first layer (full nodes) are considered triggered and known, while the leaves (empty nodes) are considered new. All links are regarded as new (represented as dashed). The choice of this tree has been done to ensure that the triggering of new edges finds nodes that are already known by the random walker.

Therefore, the first initial network we consider is made by a root, considered triggered, connected to $v_1 + 1$ new nodes. The second one adds another level to the first one. Therefore, it is a regular tree with branching size $(v_1 + 1)$ and 2 levels. Here, the root and the first level are considered triggered, while the leaves are still new. This structure is the same used in the simulations of the main text (see also Fig. S8). Finally, the third one adds one more level, thus being much bigger than the previous ones. In the panels we show only two sets of parameters, but we find comparable results for other choices of the parameters. For both sets of parameters, we find that by increasing the number of levels (and hence the number of nodes and links) in the initial network, the higher-order Heaps' exponents slightly increase. Moreover, the bigger the network, the longer we see a transient time in which there is a much higher Heaps' exponent. For example, see the blue line in Fig. S7(a), where we can clearly find the initial higher slope. Nevertheless, notice that after this period, the pace of discovery, i.e., the exponent, seems to be similar across different initial conditions, thus showing that the initial structure of the network is not relevant for the asymptotic behaviour of the ERRWT model.

Now, using Eq. (S40) and Eq. (S41), we are able to work out an analytical expression for the two exponents β_1 and β_2 . Let us consider various cases. First, assuming a sublinear regime for D_2 (so that it can be neglected with respect to t), in the large time limit we can further simplify the equations and get

$$\frac{dD_1}{dt} \approx \frac{v_1 D_1}{\rho t}, \quad (\text{S42})$$

$$\frac{dD_2}{dt} \approx \frac{(v_1 + 1)D_1 + v_2 D_2}{\rho t}. \quad (\text{S43})$$

Solving both of these equations, we obtain an explicit expression for the two exponents β_1 and β_2 ; in the sublinear case we hence have asymptotically

$$\beta_1 = \frac{v_1}{\rho} \quad , \quad \beta_2 = \max\left(\frac{v_1}{\rho}, \frac{v_2}{\rho}\right) \quad (\text{S44})$$

From the expression of β_1 and β_2 in Eq. (S44), we get that the sublinear regime holds only if $v_1 < \rho$ and $v_2 < \rho$.

Before moving on to the other regimes, let us notice that β_2 is constrained to be at most equal to $2\beta_1$. This is because if the number of nodes available to explore in the network is $O(N)$, then the number of available edges is $O(N^2)$. This means that D_2 can at most grow as the square of D_1 in the large time limit, imposing a constraint on the related exponents. Let us now consider the case in which D_2 grows linearly in time, but not D_1 . Notice that this can happen only provided that $v_1 > \rho/2$; in fact, since β_2 is constrained to be smaller or equal than $2\beta_1$, then it would not be possible for β_2 to be equal to 1 if $\beta_1 = v_1/\rho < 1/2$. This regime can be obtained substituting a linear expression for $D_2 \sim at$ into Eq. (S41). In this case, if we assume a sublinear behaviour for D_1 , we can neglect the second term in the numerator, obtaining

$$\frac{dD_2}{dt} \approx \frac{v_2 at}{\rho t + (v_2 + 1)at} = \frac{v_2 a}{\rho + (v_2 + 1)a} = a \quad \implies \quad a = \frac{v_2 - \rho}{(v_2 + 1)}, \quad (\text{S45})$$

thus showing that the condition for this regime to exist is $v_2 > \rho$, otherwise the coefficient a would be negative. Then, we can substitute $D_2 = \frac{v_2 - \rho}{(v_2 + 1)}t$ into Eq. (S40), to get the actual value of β_1 :

$$\frac{dD_1}{dt} \approx \frac{v_1 D_1}{\rho t + (v_2 - \rho)t} = \frac{v_1 D_1}{v_2 t} \quad \implies \quad \beta_1 = \frac{v_1}{v_2}. \quad (\text{S46})$$

Therefore, D_1 keeps growing sublinearly provided that $v_1 < v_2$. Notice that in this case there are no conditions on the value of v_1 , which can also be larger than ρ . Reminding also the network constraint $\beta_2 \leq 2\beta_1$, we have that this regime holds provided that $\beta_1 > 1/2$, which means $2v_1 > v_2$.

Finally, there is one last regime, in which both D_1 and D_2 are linear, i.e., with exponents $\beta_1 = \beta_2 = 1$. Substituting the two linear expressions $D_2 \sim at$ and $D_1 \sim bt$ in Eq. (S40) and Eq. (S41), we obtain the following system of equations

$$\begin{cases} \frac{dD_1}{dt} \approx \frac{v_1 b}{\rho + (v_2 + 1)a} = b \\ \frac{dD_2}{dt} \approx \frac{(v_1 + 1)b + v_2 a}{\rho + (v_2 + 1)a} = a \end{cases} \quad (\text{S47})$$

from which we can work out the values of the two coefficients:

$$a = \frac{v_1 - \rho}{(v_2 + 1)} \quad b = \frac{(v_1 - \rho)}{(v_2 + 1)} \frac{(v_1 - v_2)}{(v_1 + 1)}, \quad (\text{S48})$$

which give the conditions $v_1 > \rho$ and $v_1 > v_2$ for this regime to hold. This comes out from the fact that, as we have seen before, whenever $v_2 > v_1$ we have a sublinear regime for D_1 .

Summarizing the predicted exponents for the directed version of the model for any choice of the parameter v_1, v_2 and ρ , we have:

$$\begin{cases} v_2 < \rho, v_1 < \rho & \beta_1 = \frac{v_1}{\rho}, \beta_2 = \min\left(\max\left(\frac{v_1}{\rho}, \frac{v_2}{\rho}\right), \frac{2v_1}{\rho}\right) \\ v_2 \geq \rho, v_1 \leq \frac{\rho}{2} & \beta_1 = \frac{v_1}{\rho}, \beta_2 = \frac{2v_1}{\rho} \\ v_2 \geq \rho, \frac{\rho}{2} < v_1 < v_2 & \beta_1 = \frac{v_1}{v_2}, \beta_2 = 1 \\ v_1 \geq \rho, v_1 \geq v_2 & \beta_1 = \beta_2 = 1 \end{cases} \quad (\text{S49})$$

The results above give us an analytical overview of a simplified version of the model, which can still provide the phenomenology we are interested in. In fact, with this analysis we still obtain a different behaviour for D_1 and D_2 with two different Heaps' exponents β_1 and β_2 , which are controlled by the parameters v_1 and v_2 , given ρ .